INL/EXT-21-64543
Revision 0

FY21 Progress Report for Advanced Re-fabrication/Re-instrumentation Capability Development (M2FT-21IN020402037)

September 2021

Jason Schulthess, Connor Woolum, Joe Palmer, Kevin Terrill, Connor Michelich, Spencer Parker, Collin Knight, Colby Jensen, Mark Cole

Idaho National Laboratory

INL is a U.S. Department of Energy National Laboratory operated by Battelle Energy Alliance, LLC

INL/EXT-21-64543
Revision 0

FY21 Progress Report for Advanced Re-fabrication/Re-instrumentation Capability Development (M2FT-21IN020402037)

September 2021

Idaho National Laboratory
Nuclear Science & Technology
Idaho Falls, Idaho 83415

http://www.inl.gov

Prepared for the
U.S. Department of Energy
Office of Nuclear Energy
Under DOE Idaho Operations Office
Contract DE-AC07-05ID14517

Page intentionally left blank

ABSTRACT AND ACKNOWLEDGEMENTS

In support of performing follow on irradiation experiments with previously irradiated materials, the Halden Reactor Project developed unique and state of the art capabilities to refabricate and re-instrument previously irradiated materials. Such materials were used in in-pile tests at the Halden reactor, and out-of-pile tests for example using furnaces as a heat source. The decision to close the Halden Reactor Project results in the loss of this refabrication and re-instrumentation capability. As a result, the United States Department of Energy has determined to develop refabrication and re-instrumentation capability at the unique shielded facilities at Idaho National Laboratory. The development of refabrication capability has been completed and demonstrated. This report focuses on the complementary aspects of re-instrumentation and the progress to-date. Halden spent nearly 30 years developing both refabrication and re-instrumentation. Collaboration with Halden is allowing INL to develop this capability much more rapidly. The results include development of the capability to drill annular center holes in ceramic UO2 fuel pellets, development of fuel rod end caps with feedthroughs for centerline instrumentation inside the rodlet, The procurement of both fuel drilling and welding demonstration equipment from Halden, evaluation of surface thermocouple attachments to support better understanding of temperature measurement uncertainties, and finally, the conceptual design of a new shielded enclosure where advanced refabrication and re-instrumentation equipment can be housed.

The authors would like to thank the numerous colleagues at INL and Halden who provided support in accomplishing this work. Their support both material and intellectual is invaluable in advancing the state of the art and establishing the capabilities for refabrication and re-instrumentation at INL.

Page intentionally left blank

CONTENTS

FIGURES

TABLES

Page intentionally left blank

ACRONYMS

ATF	accident tolerant fuel
ATR	Advanced Test Reactor
CT	Computed Tomography
EFF	Experimental Fuels Facility
EPIC	Experiment Preparation and Inspection Cell
GTAW	Gas Tungsten Arc Welding
HBWR	Halden Boiling Water Reactor
HFEF	Hot Fuel Examination Facility
HIP	Hot isostatic press
HRP	Halden Reactor Project
IFE	Institue For Energy Technology
INL	Idaho National Laboratory
LI	Laboratory Instructions
LWR	Light water reactor
OD	Outer Diameter
PWR	pressurized-water reactor
SAR	Safety Analysis Report
TC	Thermocouple
TREAT	Transient Reactor Test Facility
WUPS	Weld Under Pressure System

Page intentionally left blank

FY21 Progress Report for Advanced Re-Fabrication/Re-Instrumentation Capability Development (M2FT-21IN020402037)

1. Introduction

The Halden Boiling Water Reactor (HBWR) in Norway and its international collaborative research program, the Halden Reactor Project (HRP), were, until their recent closure, a key resource for assessing nuclear fuel and materials behaviors to address issues and answer regulatory questions supporting the light-water reactor (LWR) community. HBWR and HRP included significant experimental capabilities and knowledgeable staff developed over decades to perform this challenging work. Recognizing a potential challenge induced by the closure of HBWR, a gap assessment was performed to identify critical capabilities historically provided by HBWR and develop recommendations for filling those capability gaps to support the ongoing Accident Tolerant Fuel (ATF) Program. (Jensen et al. 2018)

The gap assessment highlights four key capabilities/recommendations for investment:

- Acceleration of loss-of-cooling accident testing at the Transient Reactor Test (TREAT) Facility
- Expansion of the water loop and ramp testing capability at the Advanced Test Reactor (ATR)
- Establishment of refabrication/instrumentation capability
- Deploy reliable advanced in-pile instrumentation.

This report will focus on progress and development in the establishment of the refabrication and instrumentation capability at Idaho National Laboratory (INL).

Refabrication and instrumentation is considered an enabling capability that allows access to fuel materials at any point in their lifecycle. It is also critical in supporting the deployment and qualification of ATF materials, as many candidate materials are already undergoing irradiation as lead test rods in commercial nuclear power plants, and irradiation in ATR alone cannot produce the quantities of materials necessary to support qualification.

Refabrication and instrumentation allows for the use of the lead test rod materials that have been irradiated under prototypic commercial conditions, including localized phenomena like fretting, grid spacer effects, and corrosion. Specific segments of these materials can then be selected for subsequent testing under steady-state, transient, or ramp conditions. Refabrication also allows instrumentation to be added to these segments to measure parameters, such as temperature and fission gas release.

Halden first successfully re-instrumented a fuel rod segment for subsequent follow-on irradiation testing in 1991 and performed refabrication and instrumentation on more than 130 rod segments during operations over the next 25+ years. During this time, Halden further refined this capability and developed significant staff expertise.

INL has selected a phased approach to refabrication and instrumentation in which efforts were primarily focused on establishing a “basic refabrication” capability initially, with initial scoping efforts for “advanced re-instrumentation” proceeding in parallel.

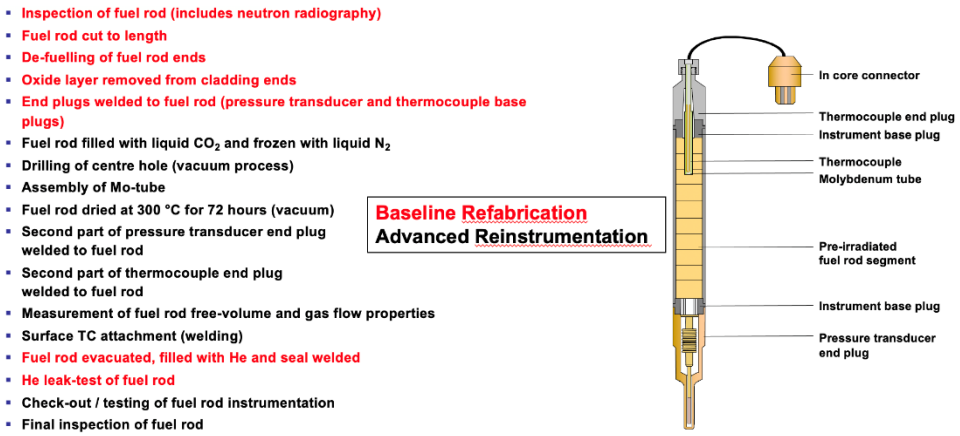

Figure 1. Shows the distinction between basic refabrication activities and advanced re-instrumentation.

During FY-21, INL successfully completed the development and installation of all basic refabrication equipment into the Hot Fuel Examination Facility (HFEF) and successfully demonstrated basic refabrication on an irradiated fuel rod from the ATF-2 experiment.

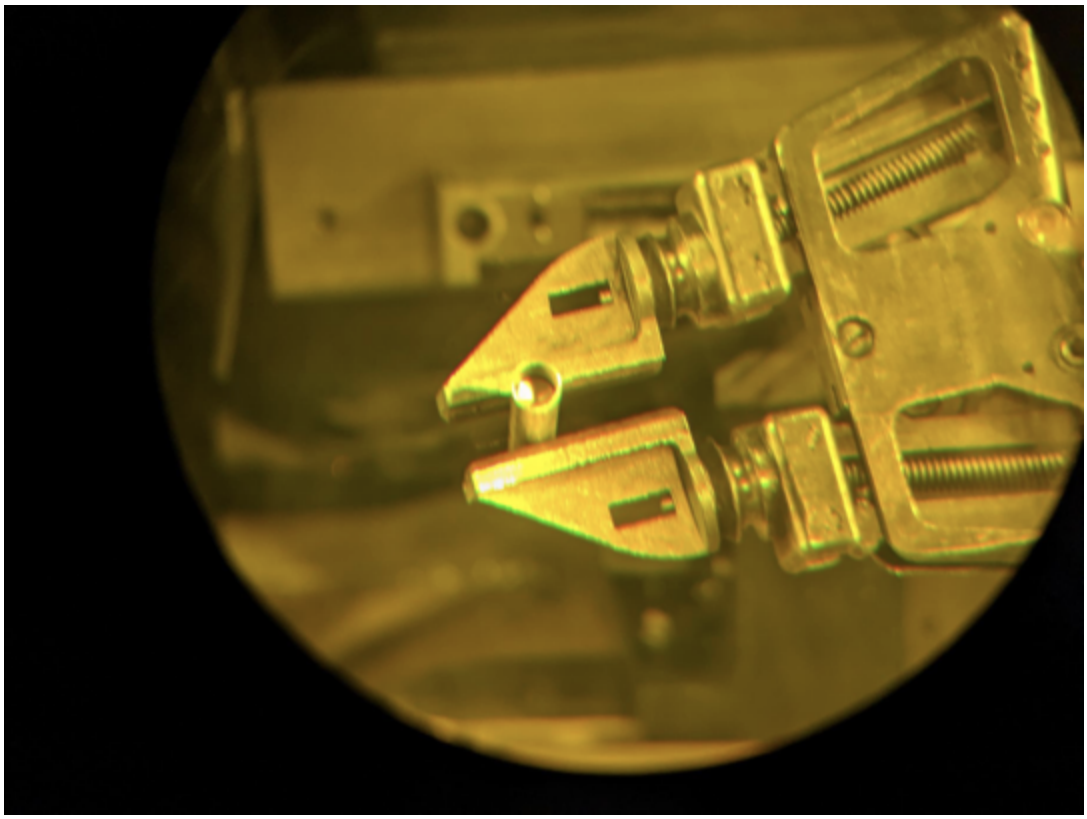

Figure 2. The fuel rod segment after defueling the ends of the segment to make space for new end caps to be inserted.

The remainder of this report will focus on the initial scoping efforts to develop advanced re-instrumentation capabilities.

Scoping studies for pellet drilling have been divided into two subsections and include efforts to perform dry drilling on fresh fuel pellets and a "cryo-drilling" technique technology transfer via a collaboration with Halden. The demonstration of the dry drilling technique was ultimately successful and allowed for the assembly of a first fresh fuel rodlet with a centerline hole and a thermocouple.

Endcaps for rodlets that support instrumentation are non-trivial and are highly experiment specific. Initial scoping studies were performed to develop an endcap that could support a centerline fuel thermocouple were completed and also supported the assembly of a first fresh fuel rodlet with a centerline thermocouple.

Previous work done at both INL and Halden indicated that temperature measurements by thermocouples attached to the outer surface of fuel cladding are sensitive to a number of parameters, including attachment method, mechanical design, spacing, fin effect, two phase flow, etc. To better understand some of these sensitivities, we performed modeling of the thermocouples, and it is being used to inform work to weld thermocouples to cladding outer surfaces.

Thermocouples mounted to the exterior surface of fuel cladding have historically proven to be some of the most useful data collected from in-pile experiments. Despite demonstrated success at INL in attaching thermocouples to cladding for fresh fuel TREAT experiments, significant challenges exist in remotely attaching thermocouples on previously irradiated fuel. Some initial scoping studies have been performed using the same circumferential welding system developed in the basic refabrication work. Initial work shows that thermocouples can be attached to cladding surfaces using this welding system. However, a method to hold thermocouple leads in place for remote welding and the optimization of the welding process remain a challenge.

A dedicated shielded enclosure facility continues to be identified as the preferred option for the long term use of advanced refabrication and re-instrumentation work. In support of this, preconceptual engineering design activities were continued to develop the design of a dedicated refabrication and advanced re-instrumentation cell, should funding become available in the future.

Each of these scoping areas to support advanced re-instrumentation will be discussed in more detail in the following sections.

2. Dry Pellet Drilling Development

Fuel centerline temperature measurements during irradiation testing are critical to understanding fuel performance. This holds true for steady-state irradiations and especially true for transient conditions, where fuel specimens are driven to failure and in-situ data can inform the failure threshold and mechanisms that may not be readily apparent during follow-on destructive post-irradiation examination. However, instrumenting a fuel rod to allow for fuel centerline temperature measurements introduces many challenges.

In the case of pre-irradiated fuel rods, the specimen must be sectioned to length and de-fueled on both ends to allow the welding of an endplug to the test specimen. Fuel pellets within one end must be drilled out to accommodate a thermocouple in the center annulus. The thermocouple must be fed through some form of endplug suitable for welding to the fuel specimen and also capable of forming a leak-tight seal around the thermocouple. All these tasks pose mechanical challenges, which are further complicated as a result of the highly radioactive specimen, thus requiring all operations to be performed remotely within a hot cell.

Until recently, equipment required to conduct all of these requisite operations did not exist at INL. The HFEF contained a mill, and a lathe welding system for welding endplugs was deployed as part of the basic refabrication effort. The existing mill within HFEF was determined to likely be suitable for defueling efforts required to refabricate irradiated specimens; however, it was unknown if the mill would be suitable for creating an annulus within fuel pellets. [IAEA, 2009]

In addition to increased demand for the capabilities to refabricate irradiated fuel rods, the need for instrumented fresh fuel rodlets has increased as well, including rodlets with fuel centerline thermocouples. As a result, a significant effort has been invested in developing a technique suitable for drilling ceramic fuel pellets. These studies ultimately support multiple different end goals, including the capability to machine fresh fuel pellets to accept a centerline thermocouple, and also information relating to pellet-drilling technique and its suitability for application within a hot cell using either existing equipment or a new benchtop and readily deployable equipment.

Initial drilling efforts focused on using surrogate material in lieu of UO_2 pellets and making use of existing laboratory equipment. The Experimental Fuels Facility (EFF) houses multiple machining technologies, including lathes and mills, and the accompanying infrastructure necessary to machine on specimens containing radiological material and on radiological specimens themselves. These EFF capabilities are limited to fresh fuel specimens only. Cerium oxide (CeO_2) was initially used as a surrogate for UO_2 fuel pellets in an attempt to develop a process before transitioning to actual fuel pellets.

Initial drilling tests were based on replicating conditions reported by [IAEA, 2009] and the suggested use of a diamond drill tube at high rotational speed of 10,000 rpm. Unfortunately, none of the existing machining equipment available for this development effort were suitable for 10,000 rpm rotational speeds; however, the hollow diamond drill tubes served as a starting point. A HAAS TL-1 lathe was first used in conjunction with these hollow bits and ceria pellets, drilling at a much lower 1,500 RPM and 0.010-in. peck rate. It was immediately discovered that the hollow bits rapidly clogged after every peck, requiring the operator to clean the core of the bit out frequently.

Follow-on efforts using a hollow-core drill made use of a UMC 750 mill located at the Materials and Fuels Complex machine shop. While the machine shop is not suitable for the drilling of fuel specimens, the intent was to test the selected drill bits at a higher rotational speed. Drilling ceria pellets at 5,000 rpm results in the total fragmentation of the pellets. At this point, hollow-core diamond bits were abandoned, and high-speed stainless-steel bits were tested.

Making use of the TL-1 in EFF again, the high-speed stainless-steel bit was found to successfully drill individual ceria pellets; however, the drill exiting the bottom of the pellet resulted in the chipping and end-capping of the pellet. At this point, further investigation revealed that the ceria pellets, which were procured from a commercial vendor, had not been sintered. Ceria pellets were abandoned, and the switch was made to begin using commercially procured UO_2 fuel pellets.

The radiological machine shop within EFF contains a HAAS ST10 lathe and a HAAS Mini-Mill. These initial drilling efforts on UO_2 pellets focused on a higher rotational speed of 5,400 rpm and made use of diamond-coated carbide drill bits instead of high-speed stainless-steel bits. These diamond-coated carbide drill bits were found to be harder than the stainless-steel bits and yielded better results when drilling the ceramic UO_2 pellets. A 0.062-in. hole was successfully drilled within the UO_2 pellets using the ST10 lathe, although chipping and end-capping remained an issue at the drill exit point.

Multiple methods to minimize chipping as the bit exited the back of the pellets were explored. A custom-machined nylon backer was fabricated to match the profile of the bottom of the fuel pellet in an attempt to provide support during drilling. The addition of a nylon backer behind the pellet within the collet had the unintended consequence of increasing collet vibration, resulting in the complete fragmentation of the fuel pellet.

A technique to first drill a smaller diameter pilot hole was also tested. A 0.031-in. drill bit was used to machine a pilot hole within the pellet. Machining this first hole did not cause any chipping at the point the drill exited the pellet. However, when the pilot hole was drilled using the standard 0.062-in. bit, the result was still a chipping of the pellet at the drill exit point.

Utilizing the lathe, the method that ultimately proved most successful required drilling the pellet initially from one side then flipping the pellet to drill all the way through from the other side. Pellets were

drilled approximately one-quarter of their thickness prior to rotating. This did create some challenges in locating the drill on the second side of the pellet to ensure that both holes aligned properly; however, using precision gauges and indicators allowed for an adequate position alignment to drill a thru-hole within approximately 0.0005-in. or less. For the purposes of this effort, this small positional difference was determined to be inconsequential. Furthermore, when drilling the pellet from the second side, the pellet is still drilled completed through, resulting in a thru-hole that is at least the size of the drill bit as opposed to two mating annuli that are misaligned. It's important to note that, while chipping was minimized, some minor chipping of the pellet remained.

Drilling efforts to date had primarily focused on the rotation of the pellet specimen while the bit was held stationary. In an attempt to further increase the precision of the drilling technique and decrease any potential chipping, the Mini-Mill was exercised to drill UO_2 pellets by holding the pellet stationary and instead rotating the tool. Using the same general technique of partially drilling a pellet then rotating it to complete the annulus, this method was found to be most successful of all attempts. Drilling specifics included a tool rotation of 5,400 rpm and a tool feed rate of 0.75 in. per minute for 0.010 in. pecks.

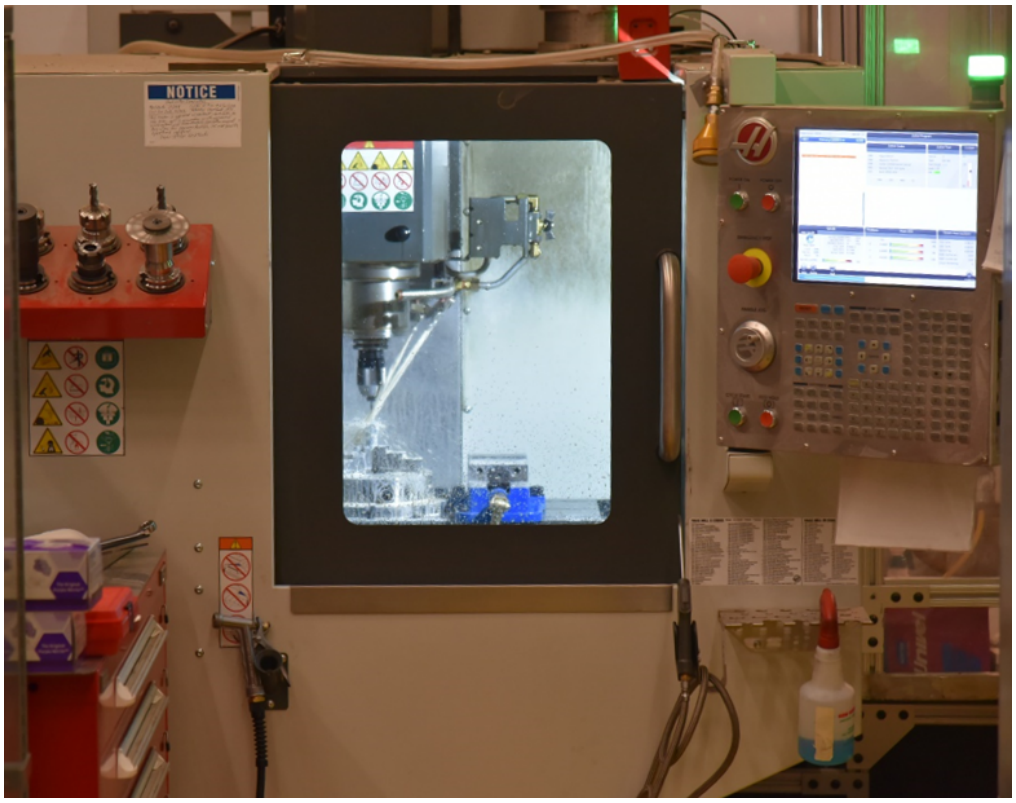

Figure 3. A UO_2 pellet is fixtured within the HAAS Mini-Mill for drilling.

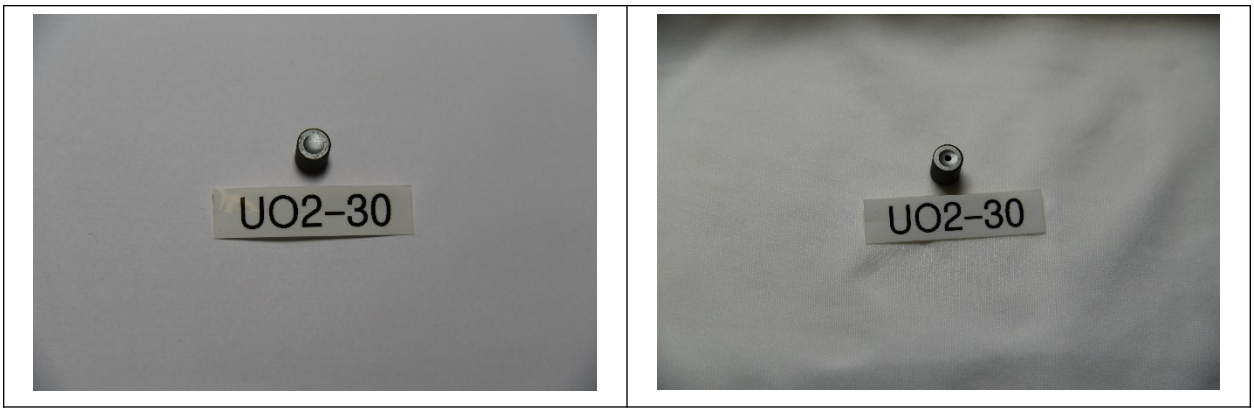

Figure 4. UO_2 pellet prior to drilling (left) and post-drilling (right).

Given the success of using the Mini-Mill in drilling through fresh UO_2 pellets, no further developments or technique modifications were explored, such as other types of drill bits or feed and speed rates. However, the existing endmill within HFEF has a spindle that is limited to 3,000 rpm. Additional tests using fresh fuel in the Mini-Mill proved successful at a decreased drill speed of 3,000 rpm, yielding similar results as pellets drilled at 5,400 rpm. This result indicates that the HFEF endmill is at least capable of drilling UO_2 fuel pellets in the most basic sense.

In addition to the traditional mechanical drilling techniques, the use of an ultrasonic drill was tested as a means to create an annulus within a pellet. Ultrasonic drilling offers the advantage of gradually abrading material through the use of a small diameter tube in place of a standard drill bit. This technique also has the advantage of being readily deployable within a hot cell as a benchtop system with a small footprint.

A Highland Park Ultrasonic Drill, model USD-110 was procured and setup within the Advanced Fuels Facility. As an off-the-shelf piece of equipment, significant modifications would be required to allow for its application to radiological materials. The drill relies upon a constant flow of liquid with a suspension of silicon carbide as the drilling media. The unit itself does not provide protection against splashing and has controls within the area that liquid is handled, which would have to be modified and shielded before the drill could be tested using UO_2 pellets. Given the unique nature of this drilling method and the requisite equipment modifications to test drill UO_2 pellets, ceria was again used as a surrogate to test initial equipment functionality.

The test system setup required the manual handling of drilling specimens, meaning that the pellets were held using tools and manipulated against the ultrasonic bits by hand. A more robust, precise, and repeatable handling system could have been fabricated, but this would not completely eliminate issues and would still be subject to the inherent limitations of this ultrasonic technique. The test pellets also still exhibited chipping at the end of the pellet in the region where the drill bit exited the pellet. Additionally, the system would require heavy modifications to be suitable for use with radiological materials. While the drill was capable of producing a hole within the ceria pellet, the ultrasonic drill was ultimately abandoned as a viable technique for fuel pellet drilling for these reasons, with the imprecision with which holes were drilled being one of the primary reasons.

While an appropriate technique for drilling fresh fuel pellets on an individual basis was developed, any previously irradiated specimen geometry would include pellets within cladding. Depending on specimen burnup, there's the potential for some form of chemical and mechanical interaction between the fuel and pellets and also the potential for cracking of the fuel pellets. Clearly this technique of drilling from both sides of the pellet, as is suitable for fresh specimens, is not viable for irradiated specimens.

Further investigation out-of-cell on a viable technique to drill fuel pellets within their cladding requires the creation of surrogate specimens. Initial efforts to create a surrogate specimen focused on the use of a hot isostatic press (HIP) that is located within the Fuels and Applied Sciences Building. This HIP, previously used to create plate-type fuels, had sat idle for several years. As a result, the pump and

cooling jacket used to cool the HIP were inoperable. It was expected, however, that the cladding would yield at approximately 12 ksi at room temperature.

A non-fueled surrogate rodlet comprised of Zircaloy-4 cladding and endplugs was assembled, using stainless-steel slugs in place of fuel pellets. The rodlet was welded using typical laser-welding techniques to create a sealed specimen. This specimen was loaded into the HIP chamber, and the chamber subsequently pressurized to 15 ksi, the upper administrative pressure limit of the HIP.

This first test was intended to determine the viability of this HIP technique to create the necessary surrogate specimens—if the upper pressure limit of the HIP was an insufficient pressure to collapse the cladding, other techniques would need to be explored. The HIP run successfully collapsed the cladding. The surrogate rodlet was assembled with a small plenum length, that is, the steel surrogate pellets only occupied approximately 4.5 in. of the rodlet and the volume of the upper 0.5 in. contained nothing more than gas. As a result of this configuration, the entirety of the HIP-induced cladding failure occurred in the plenum region, as there was no structural support of the cladding from inside, as can be seen in Figure 5.

Figure 5. Rodlet exhibiting complete collapse of the cladding within the plenum region after HIP run.

A follow-on HIP test was designed using a rodlet that was completely filled with steel surrogate pellets. Unfortunately, the HIP experienced equipment failure during this second run, at which point these efforts to create a surrogate rodlet specimen were scaled back.

It can be reasoned, however, that this technique can be used to create viable surrogate specimens for further pellet-drilling evaluation with additional process development to determine the exact HIP operating parameters to artificially compress cladding onto pellets within.

A much more rudimentary method to create surrogate specimens included the use of epoxy to cement pellets into place. Two high-temperature epoxies, Ceramabond 569 and Ceramabond 671, were evaluated as candidates, and both ultimately proved successful. In each case, four surrogate mullite pellets were epoxied into cladding using these epoxies and allowed to cure, followed by test drilling using the Mini-Mill and the technique described above. These pellets were successfully drilled within cladding, in spite of having to drill all pellets from only one orientation and through the depth of multiple pellets. As a result of reprioritization, this effort was scaled back; however, the obvious next step is to replicate the process of epoxying pellets into place using UO_2 pellets in lieu of surrogates. This test would be expected to provide significant information regarding the viability of the mill within the HFEF hot cell to adequately drill pre-irradiated fuel specimens.

3. Dry Pellet Drilling Development

3.1 Historic Case for Cryo-Drilling and Why Halden Used This Method

More than 30 years ago, the HRP (now Institute For Energy Technology (IFE) began developing techniques for refabricating full-length irradiated fuel rods into much shorter (150–400 mm) "rodlets," which could then be re-irradiated in one of their pressurized water loops. Originally, this was done by simply shortening the rods, removing a pellet from each end, cleaning the oxide off the Zr-4 cladding from each end, and welding on new Zr-4 end caps. However, there was a desire to monitor temperature during irradiation. It was recognized that this would require drilling a center hole in the irradiated UO_2 ceramic approximately 50-mm deep in order to accommodate a thermocouple.

They determined that it was possible to dry drill a hole in the UO_2 ceramic using a hollow, diamond-tipped bit. Drilling dry required that they go slow and potentially replace the bit during the process. However, the difficulty was that, once irradiated at a high temperature, the UO_2 pellets are no longer solid entities but rather severely fractured. In such a situation, the drill is not working its way through solid material but rather something akin to a gravel bed. IFE discovered that, when the bit completed its work and was removed, the gravel bed would collapse on itself, making it impossible to install a thermocouple.

IFE engineers found an ingenious solution to the collapsing bed problem. They first filled the rodlet with liquid CO_2,[a] and then froze that CO_2 into a solid by filling the surrounding chamber with liquid nitrogen. With the liquid nitrogen surrounding the now frozen CO_2, the rodlet pressure could be dropped to atmospheric, which would then allow drilling to take place as before. With the UO_2 bed stabilized by the frozen CO_2, when the drill bit was removed, the hole stayed intact, and at this point, a thin-walled molybdenum tube was inserted into the hole. With the hole now sleeved, the LN_2 and CO_2 could be allowed to evaporate (technically, sublimate in the case of the CO_2).

Molybdenum was selected as the sleeving material because it has a very high melting temperature and it is inert to both the UO_2 ceramic and the niobium-sheathed high-temperature thermocouple, which had been selected to measure the temperature.

3.2 Technology Transfer from IFE to INL

The closure of the Halden reactor was a major loss to the worldwide LWR fuels and materials research and development community, especially at a time when such test facilities are increasingly scarce. The DOE has a stated goal to capture or preserve as many of IFE's technological innovations as possible. One of these technologies is their fuel rodlet re-instrumentation process. The process consists of three major operations: defueling of rodlets (i.e., removal of a pellet from each end and removal of oxides near what will be the weld surfaces); drilling and installing a thermocouple or other relevant sensor; and filling the rodlet with inert gas and welding it closed.

IFE accomplished these three phases by developing three equipment modules: a defueling module, a drilling module, and a welding module. INL has subcontracted with IFE to fabricate and deliver copies of these three equipment modules. As of August 2021, the defueling and drilling modules were on site, with the equipment module expected by the end of September 2021.

Note that, although this equipment was designed for hot cell use, this particular set will never be moved into a hot cell; but rather, it will be used as a test bed to first understand and practice IFE's techniques and second to develop methods for incorporating advanced instrumentation into irradiated fuel rodlets, and, hopefully, to simplify certain aspects of the IFE process.

[a] This has to be done inside a sealed chamber because CO_2 is a liquid at room temperature only under pressure. A pressure of 850 psi is required to maintain CO_2 in the liquid state at 70°F.

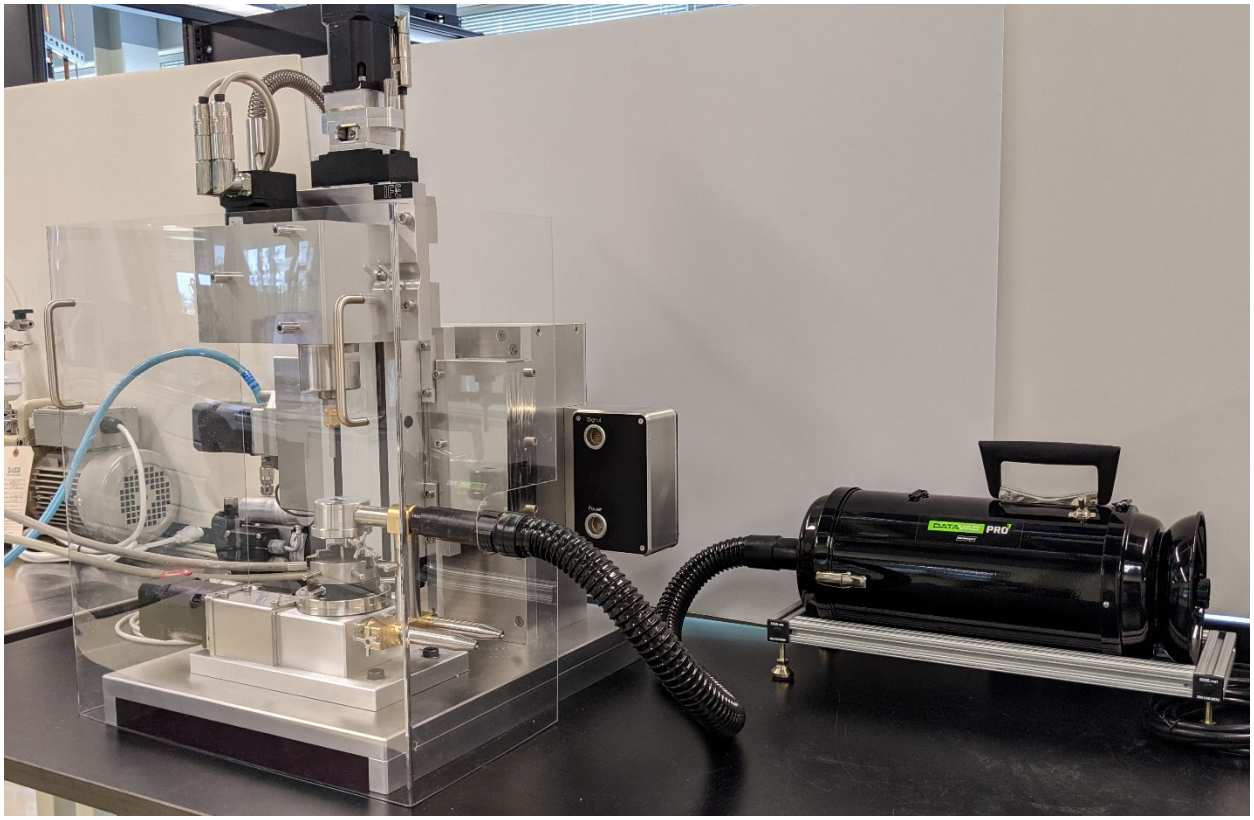

(a)

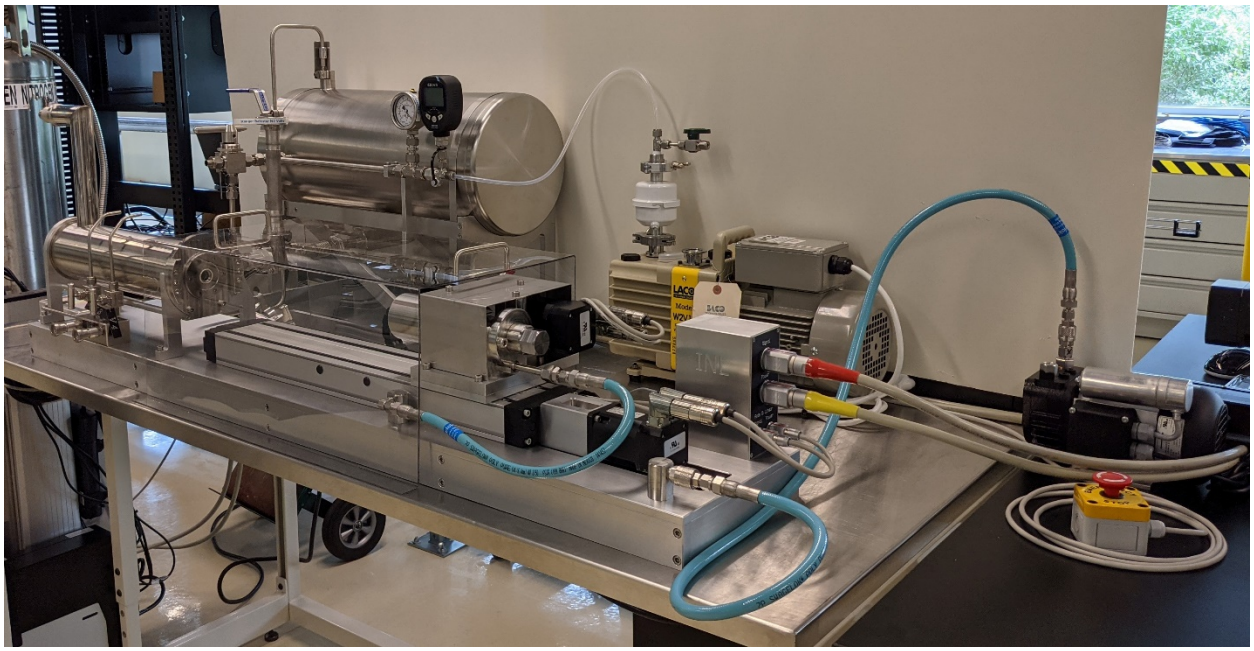

(b)

Figure 6. (a) “Defueling” module with guard and vacuum pump integrated and (b) cryo-drilling unit with vacuum pumps and guards in place.

INL received the drilling and defueling modules in February 2021. However, the formal checkout of these modules was delayed for several months, as the Laboratory Instructions (LI) developed for operating this equipment were subjected to INL's detailed safety review process. An image of the first page of the LI supporting this document is shown below in Figure 7.

This is pertinent moving forward in that it illustrates the rigor of the INL safety review process. Incorporating this equipment into the HFEF hot cell environment would require considerable time and resources.

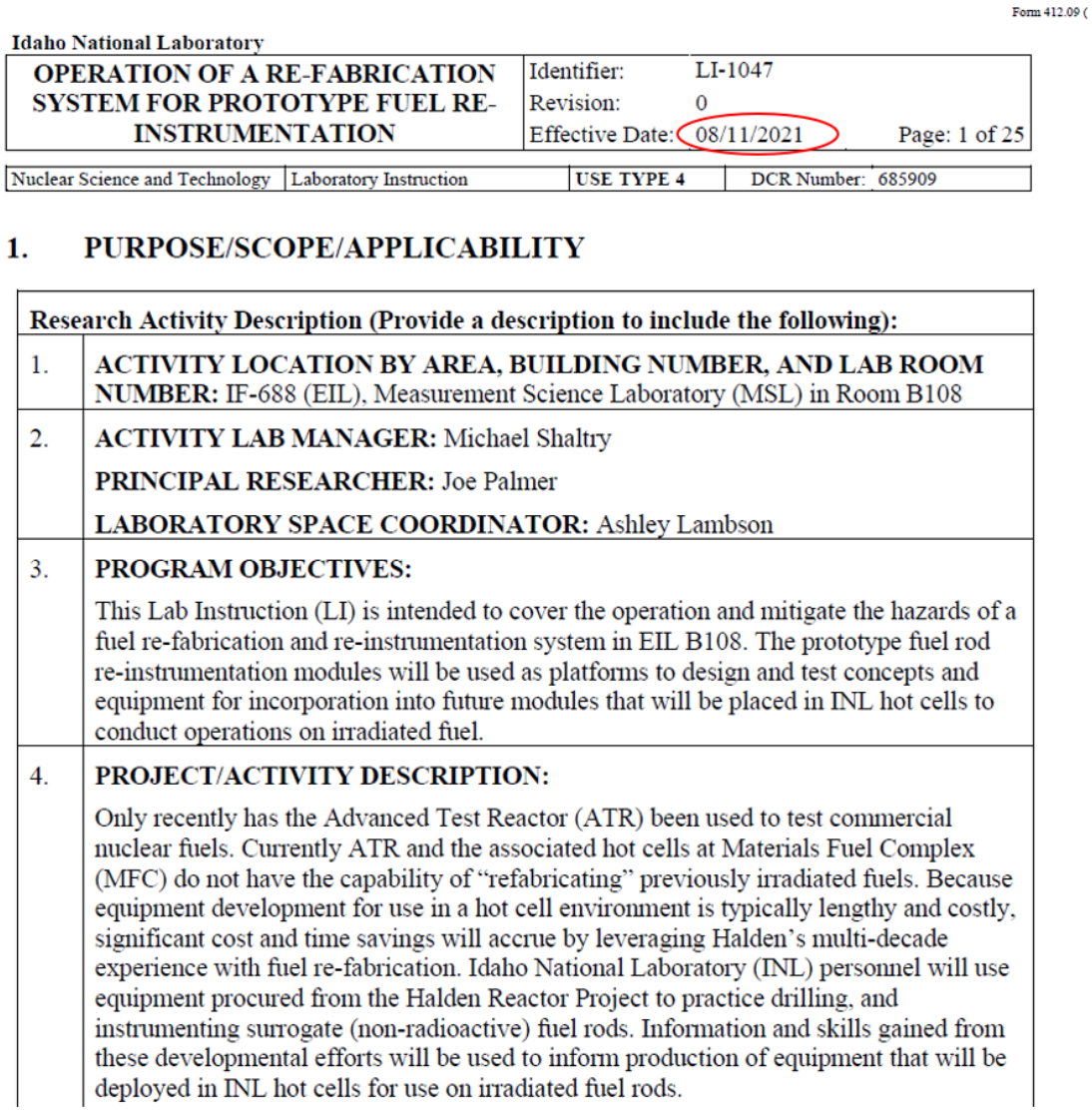

Form 412.09 (

Idaho National Laboratory

OPERATION OF A RE-FABRICATION SYSTEM FOR PROTOTYPE FUEL RE-INSTRUMENTATION	Identifier: LI-1047 Revision: 0 Effective Date: 08/11/2021	Page: 1 of 25

Nuclear Science and Technology	Laboratory Instruction	USE TYPE 4	DCR Number: 685909

1. PURPOSE/SCOPE/APPLICABILITY

Research Activity Description (Provide a description to include the following):	
1.	**ACTIVITY LOCATION BY AREA, BUILDING NUMBER, AND LAB ROOM NUMBER:** IF-688 (EIL), Measurement Science Laboratory (MSL) in Room B108
2.	**ACTIVITY LAB MANAGER:** Michael Shaltry **PRINCIPAL RESEARCHER:** Joe Palmer **LABORATORY SPACE COORDINATOR:** Ashley Lambson
3.	**PROGRAM OBJECTIVES:** This Lab Instruction (LI) is intended to cover the operation and mitigate the hazards of a fuel re-fabrication and re-instrumentation system in EIL B108. The prototype fuel rod re-instrumentation modules will be used as platforms to design and test concepts and equipment for incorporation into future modules that will be placed in INL hot cells to conduct operations on irradiated fuel.
4.	**PROJECT/ACTIVITY DESCRIPTION:** Only recently has the Advanced Test Reactor (ATR) been used to test commercial nuclear fuels. Currently ATR and the associated hot cells at Materials Fuel Complex (MFC) do not have the capability of "refabricating" previously irradiated fuels. Because equipment development for use in a hot cell environment is typically lengthy and costly, significant cost and time savings will accrue by leveraging Halden's multi-decade experience with fuel re-fabrication. Idaho National Laboratory (INL) personnel will use equipment procured from the Halden Reactor Project to practice drilling, and instrumenting surrogate (non-radioactive) fuel rods. Information and skills gained from these developmental efforts will be used to inform production of equipment that will be deployed in INL hot cells for use on irradiated fuel rods.

Figure 7. Cover sheet for the LI associated with operating drilling and defueling modules in EIL Lab B108.

3.3 Challenges Associated with Incorporating a Cryo-Drilling System into HFEF

The IFE hot cells were essentially dedicated to this line of work (i.e., the preparation and examination of previously irradiated commercial LWR fuels). As such, all resources of this portion of the Institute were devoted to accomplishing this objective. Conversely, the major INL hot cells (HFEF), support a

variety of disparate programs needing different utilities, examination equipment, etc. None of the programs currently using the main HFEF argon cell use cryogenic fluids. The incorporation of a system requiring liquid nitrogen would likely require a documented safety evaluation and an update of the HFEF Safety Analysis Report (SAR). The SAR is updated annually, and if the change can be rolled into the annual update, the cost would likely be modest. However, the supporting evaluation and calculations needed for the SAR update would need to be completed approximately 6 months before the deadline for submitting the update, and the equipment modules needed to instrument fuel rodlets would require considerable physical space in HFEF. This space would have to be negotiated with other users of HFEF, and insulated transfer tubing would have to be installed through one of the existing penetrations into the main HFEF argon cell.

During FY-22, specific efforts will be directed to determining whether a SAR update is required to accommodate cryogenic fluids in the HFEF main cell and whether specific new feed-throughs will be required to support the IFE drilling and welding equipment.

4. Dry Pellet Drilling Development

4.1 Surrogates for UO_2

Since these exercises will take place in a non-nuclear laboratory, it will be necessary to use a surrogate to simulate the UO_2 fuel pellets.

Cerium oxide (ceria) has been used as a surrogate for UO_2 by many investigators. However, this selection was primarily based on ceria's similar thermophysical properties to UO_2 (e.g., its specific heat and thermal conductivity are quite similar). For drilling and welding studies, these similarities do not appear to be important. Rather hardness, compressive strength, fracture toughness, and flexural strength appear to be more meaningful properties. Furthermore, fully sintered ceria is not readily available. American Elements has declined to provide such material. Before these issues were clearly understood, INL purchased two batches of semi-green ceria from American Elements, but it was later determined that this material would be essentially useless for drilling studies because of its very low hardness and compressive strength (very similar to common chalk).

Table 1 compares several candidate surrogate ceramics to UO2. Mullite is a common, low-cost, alumina silicate ceramic which can exist in two stoichiometric forms $3Al_2O_32SiO_2$ or $2Al_2O_3\ SiO_2$. It stands out as a practical surrogate material. It is harder and stronger than unirradiated UO2, but not dramatically so, and should serve a conservative substitute for UO_2 for the planned drilling studies. "Conservative" in the sense that it should be more difficult to mill and drill than UO2.

Table 1. Properties of ceramics compared to UO_2.

	Vickers Hardness (GPA)	Comp Strength (MPA)	Frac Toughness MPA	Flexural Strength (MPA)
UO_2	7 (p.63)	950	0.9-1.2	70
Al_2O_3	18	2100	3.5	350
AlN	13	2100	2.6	320
MACOR	3.9	345	1.5	94
Mullite	10	1310	2 (3–5)	180
BN (boron nitride)	0.2	143–186	3	76–113

It is noteworthy that, although the IFE researchers did checkout their drilling and defueling equipment ex-hot cell using ceramic surrogates, they were not overly concerned about the selection of these surrogates. Much of their practice work was on Macor, which is easier to mill and drill compared to UO_2 or mullite.

4.2 Simulating Irradiated (Cracked) UO_2

As discussed above, IFE discovered that drilling irradiated and cracked UO_2 was much different than drilling fresh, solid UO_2 pellets. As such, it will be important to practice drilling into cracked ceramics. A number of investigators have developed processes for cracking UO_2 using thermal shock methods. These efforts required fairly elaborate setups. For initial drilling studies, INL measurement science engineers have decided to mechanically crack the surrogate ceramics.

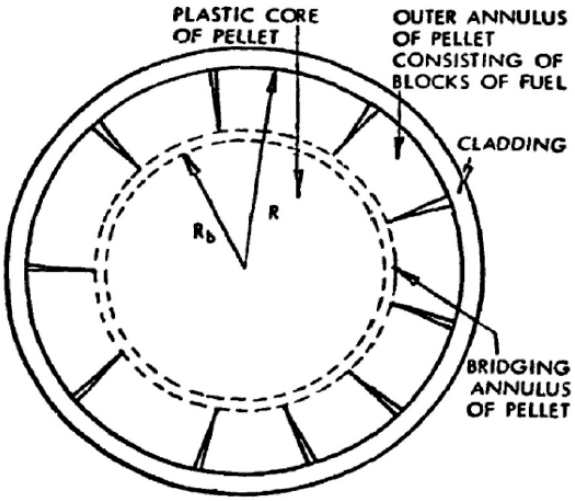

Fig. 10. Model used for crack distribution in fuel pellet [20].

Figure 8. Radial cracks on the periphery but not in the core. (Patnaik 2020)

However, Figure 9 shows that cracks can extend all the way to the pellet centerline. It's noteworthy that the macrograph shows a more random pattern, which is similar to that obtained by mechanical cracking shown in Figure 10 below.

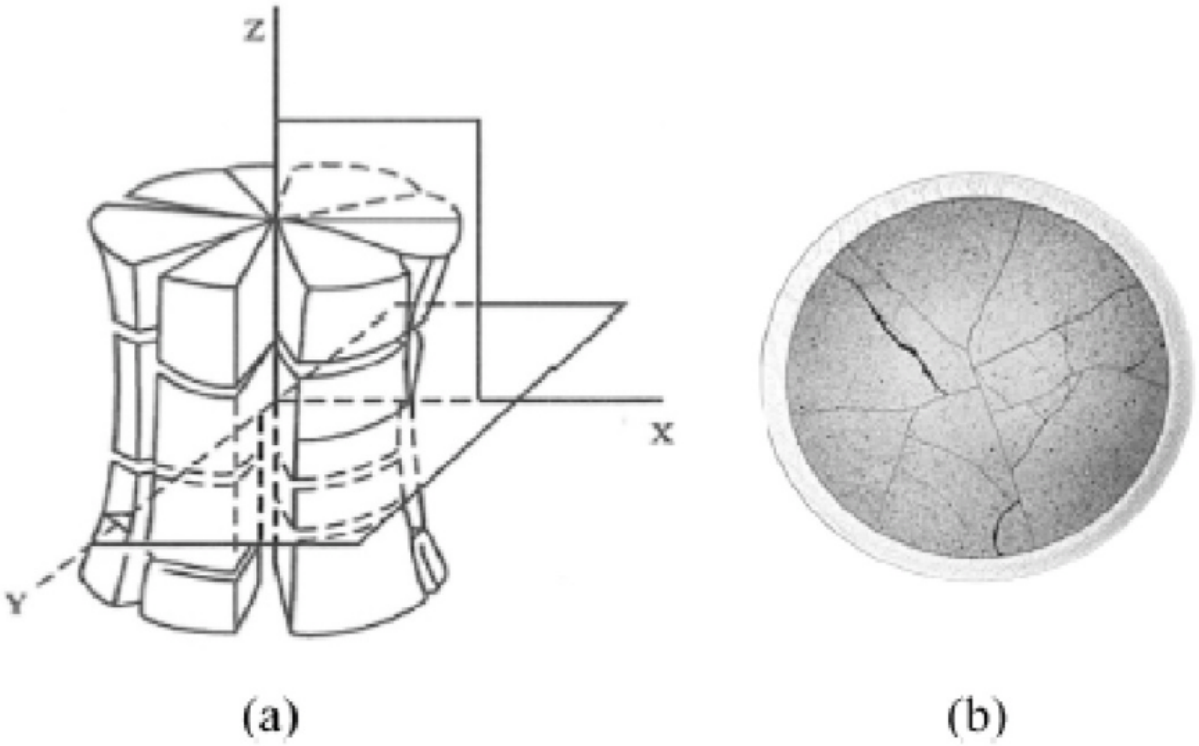

Figure 9. Cracking of fuel pellet (a) schematic of a fuel pellet with an “hour glassing” shape because of thermal stresses, (b) macrograph of a PWR fuel pellet cracked by the thermal gradient.

For the drilling study, the exact pattern of cracking does not appear to be critical to demonstrate that the equipment setup is capable of drilling cracked UO_2 pellets.

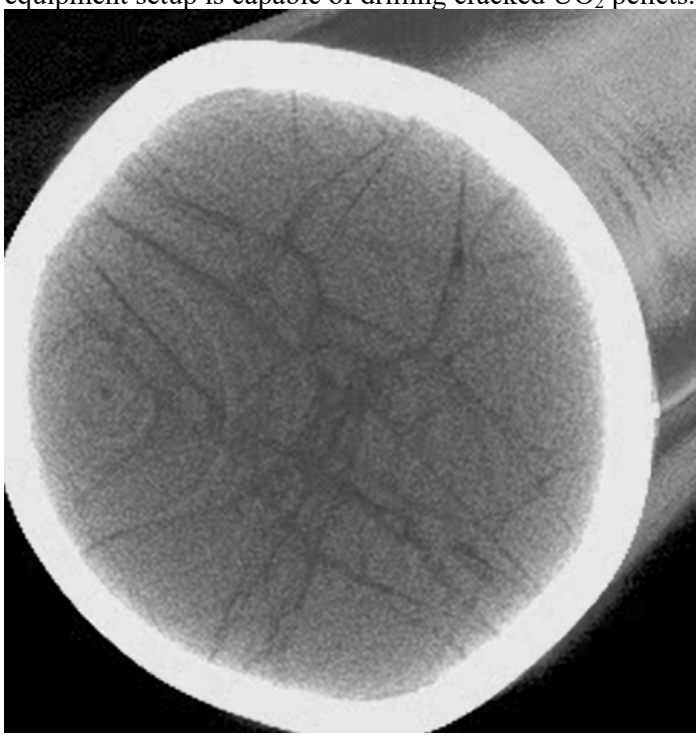

Figure 10. Computed tomography (CT) scan of mullite inside cladding, which was then mechanically cracked.

4.3 IFE Took Great Pains to Ensure Leak Tightness of Finished Instrumented Rodlets

As one studies the IFE hardware and process of instrumenting fuel rodlets, it becomes clear that preventing water ingress was a primary objective, and elaborate measures were employed to ensure leak tightness. Some of the measures they took are described below:

- After defueling both ends of a rodlet, a little subassembly was prepared for the specific purpose of separately leak checking the Zr welds involving the cladding.

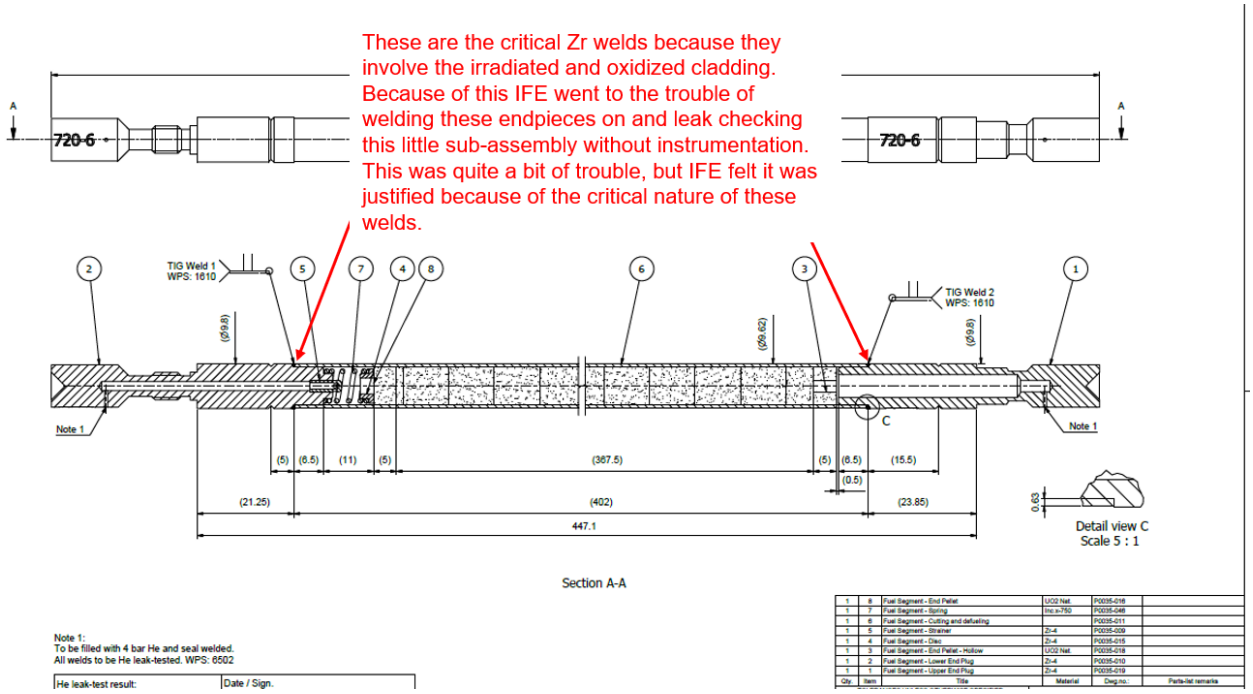

Figure 11. Initial Halden subassembly.

- After leak checking, the subassembly shown above the end pieces were parted off as shown below. Then the irradiated fuel was drilled using the cryo-system, followed by attachment of the instrumentation subassemblies as shown below.

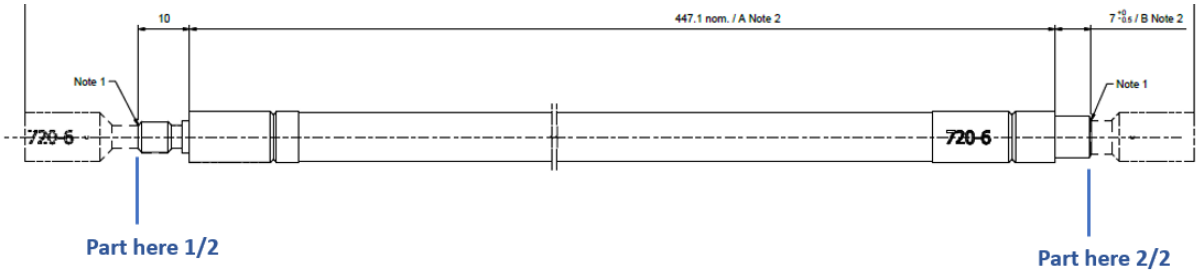

Figure 12. Second Halden subassembly.

4.4 Three Schemes for Instrumenting Irradiated Fuel Rodlets

Three schemes for installing a sensor and sealing an irradiated fuel rodlet are discussed and compared below. They are IFE, IFE as modified by INL measurement science personnel, and the INL hot cell.

Notable features of the IFE scheme are as follows (Re. Figure 11):

- IFE incorporated weep holes both above and below the fuel stack (this practice was based on the assumption of no gas path through the pellets). These weep holes are used to prevent the circumferential welds from blowing out (i.e., there must be a path for gas to escape, otherwise a circumferential weld, which seals a volume of gas, typically will blow out just as the weld is being closed).

- IFE did not use a compliant (grafoil) seal around the thermocouple cable but rather a mechanical seal: two cones forced into each other (similar to Swagelok fittings). However, unlike Swagelok fittings, IFE did not use the ferrule system, which coins a little material on the OD of the tube (TC sheath). They instead welded an I600 conical sleeve to the I600 TC sheath. This may be more complex than necessary, and INL plans to first to test the much simpler scheme featuring a Conax fitting and grafoil seal media.
- The IFE welding equipment is designed to completely enclose the rodlet and associated cabling in a pressurized, inert environment for the welding process. All the circumferential structural welds are made in this chamber followed by sealing of weepholes. Note that, in Figure 11 below the welds with the "eb" designation are not made in the hot cell, and neither are the laser welds designated "ls". These welds are pre-made on unirradiated materials outside the hotcell to create subassemblies that are then Gas Tungsten Arc Welding (GTAW) welded together within the pressurized chamber. Halden's welding scheme was much more elaborate than we are envisioning.

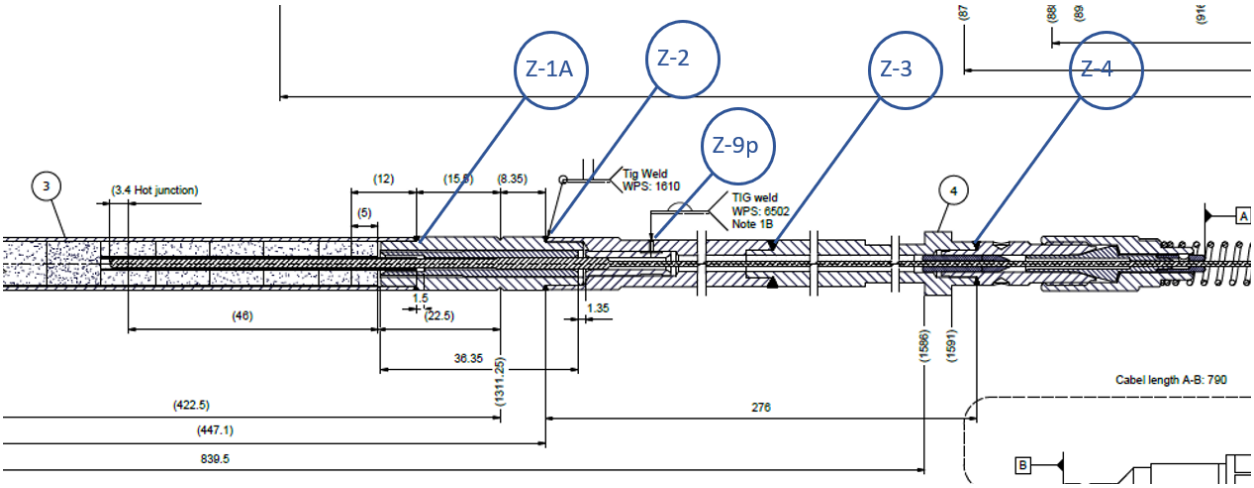

(a)

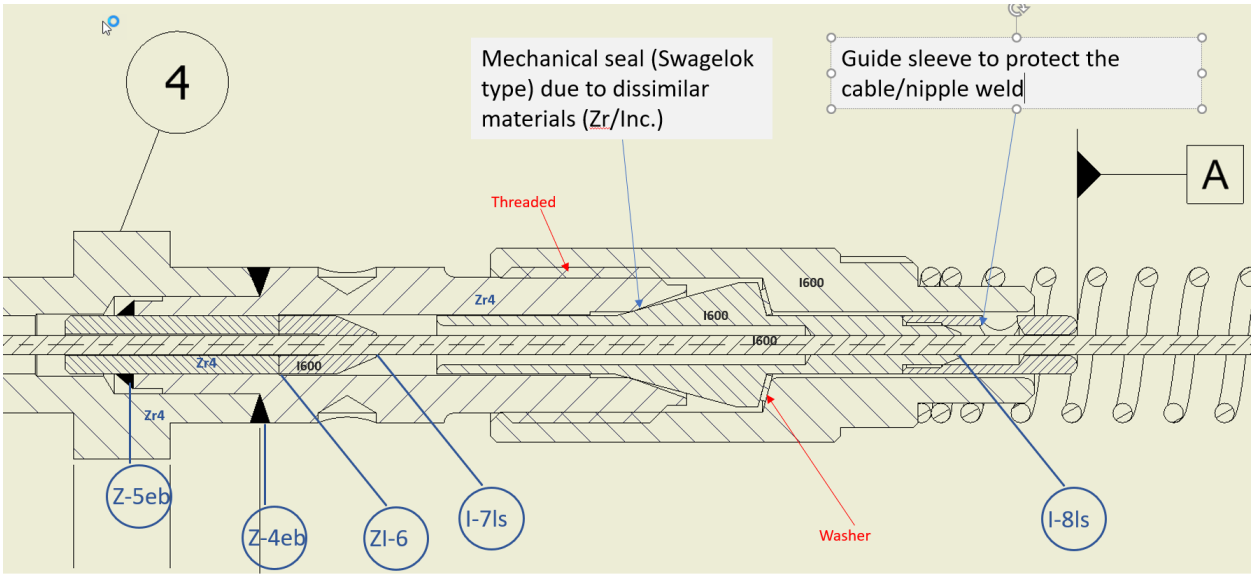

(b)

Figure 13. (a) Details of welds in IFE re-instrumentation assembly and (b) details of welds in IFE re-instrumentation assembly.

- Some of the complex features of the Halden arrangement may have been due to their unique thermocouple type, which is shown in Figure 12 below. The Halden thermocouple consists of an Inconel 600 (I600) sheathed cable that transitions to a refractory sheathed probe for the high-temperature region, which is inserted into the fuel pellet stack.

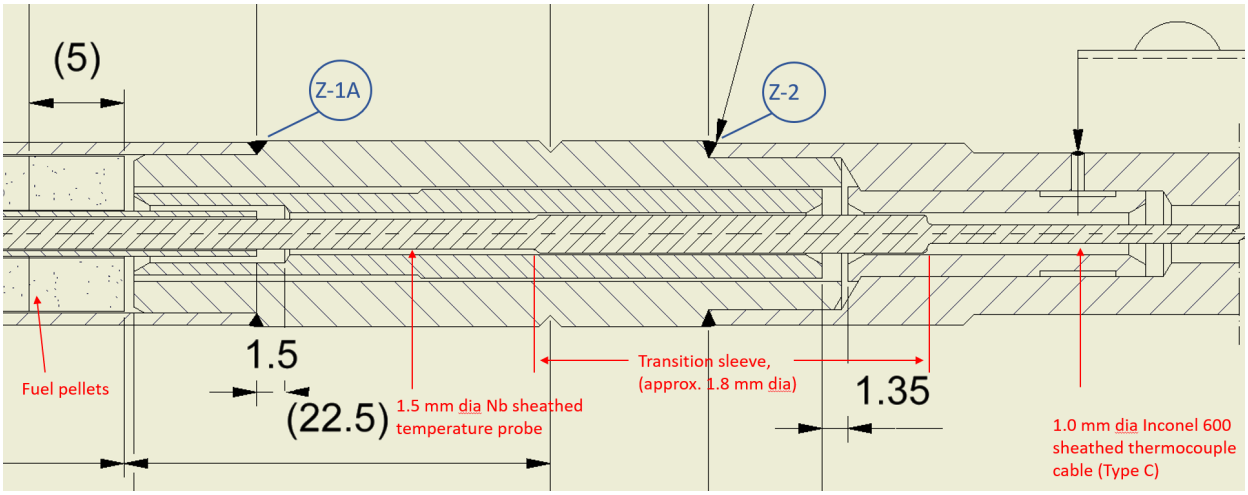

Figure 14. IFE thermocouple installation.

Notable features of the INL measurements sciences scheme are as follows (Re. Figure 13 and Figure 14):

- Similar to the IFE design, radial weep holes are incorporated into the end fittings above and below the fuel pellet stack.
- A Conax fitting with grafoil sealant is used to seal around the thermocouple cable. This is in place of IFE's mechanical seal and laser welding of cable to sealing pieces.
- Again, similar to the IFE design, the rodlet and associated cabling will be completely enclosed inside the welding chamber for the welding process. All the circumferential structural welds are made in this chamber followed by sealing of weep holes (also within the welding chamber—the WUPS system is not used with this design).
- In this case, the thermocouple consists of a double walled HTIR-TC arrangement. The outer wall is comprised of I600 alloy, which provides resistance against 300°C high-pressure loop water. Inside the rodlet, the outer sheath terminates, and only the high-temperature capable, refractory-sheathed HTIR-TC enters the fuel stack, see Figure 13 below.

An overview of the INL measurement sciences instrumented rodlet concept is shown in Figure 13 below.

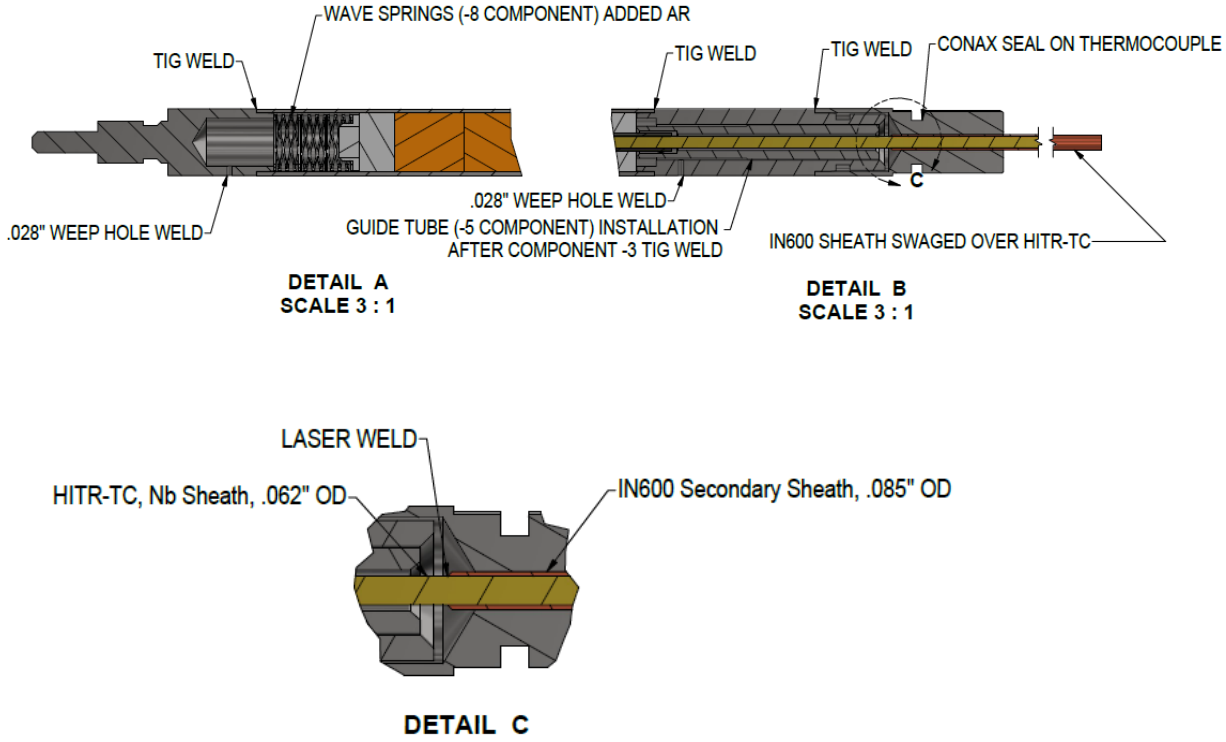

Figure 15. INL measurement sciences instrumented rodlet concept.

Figure 14 below illustrates schematically how the instrumented rodlet from Figure 13 would be incorporated into the ATR loop 2A facility.

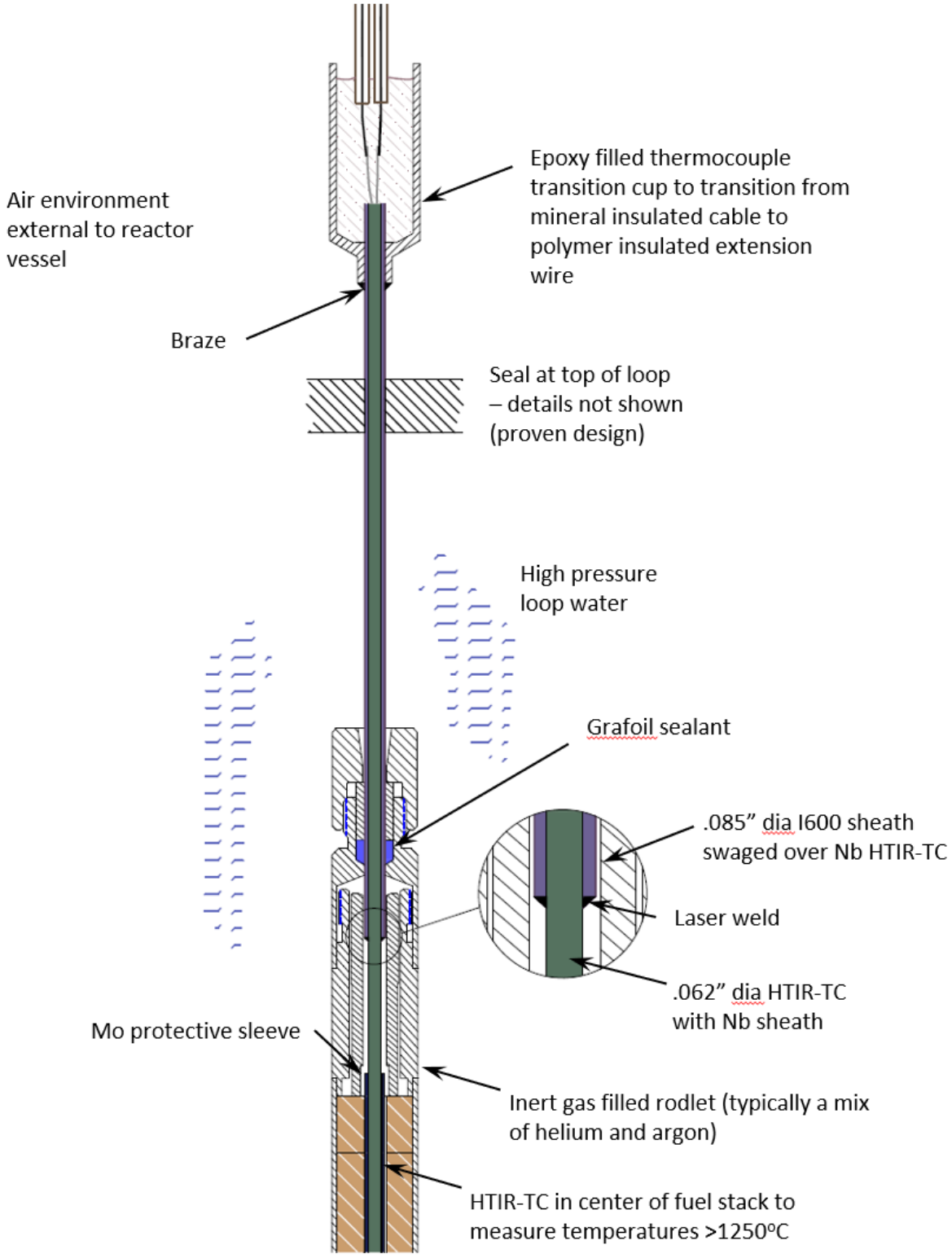

Figure 16. Salient features of INL measurement sciences instrumented rodlet installed in ATR Loop 2A.

Two failure scenarios have been postulated with respect to the dual sheathed thermocouple. The first is that fission gases could make their way between the I600 sheath and HTIR-TC cable, as shown by the red arrow path in Figure 15 below. The concern here is that these gases could exit at the transition cup above the loop seal, escape the loop environment, and discharge into the donut area above the ATR reactor top head closure plate.

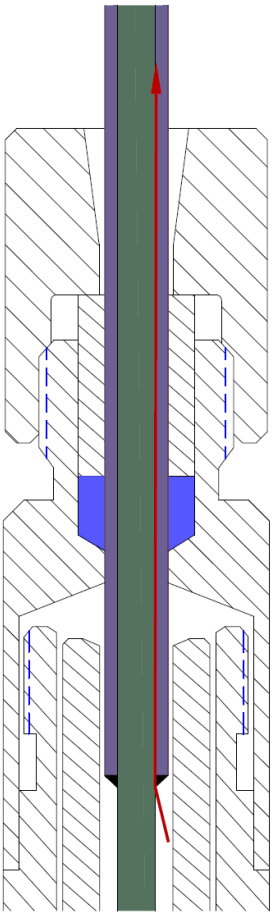

Figure 17. Postulated escape path for fission products.

Figure 16 shows three barriers designed to block the escape of fission products. The first is the weld between the I600 over-sheath and the Nb sheathed cable of the HTIR-TC. The second is the tight fit between the I600 over-sheath and the HTIR-TC, and the third is the epoxy which fills the transition cup.

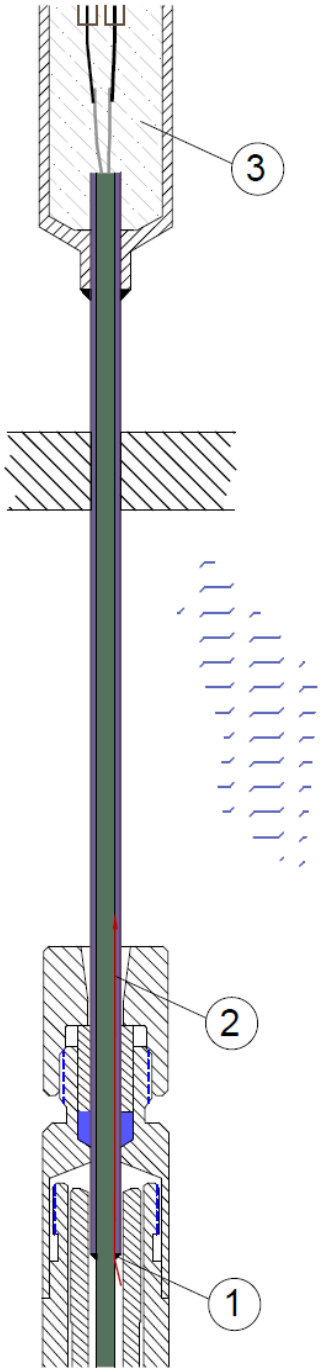

Figure 18. Barriers to the escape of fission products.

Several informal tests were conducted to determine the viability of these barriers. Figure 17 shows a photo of the I600 to Nb weld, and Figure 18 is a CT image of such a weld. In these images, the bonding between the filler (pure Ni) and the Nb looks quite good. However, a metallographic micrograph (not shown) of the weld zone showed lack of fusion between the filler and Nb sheath.

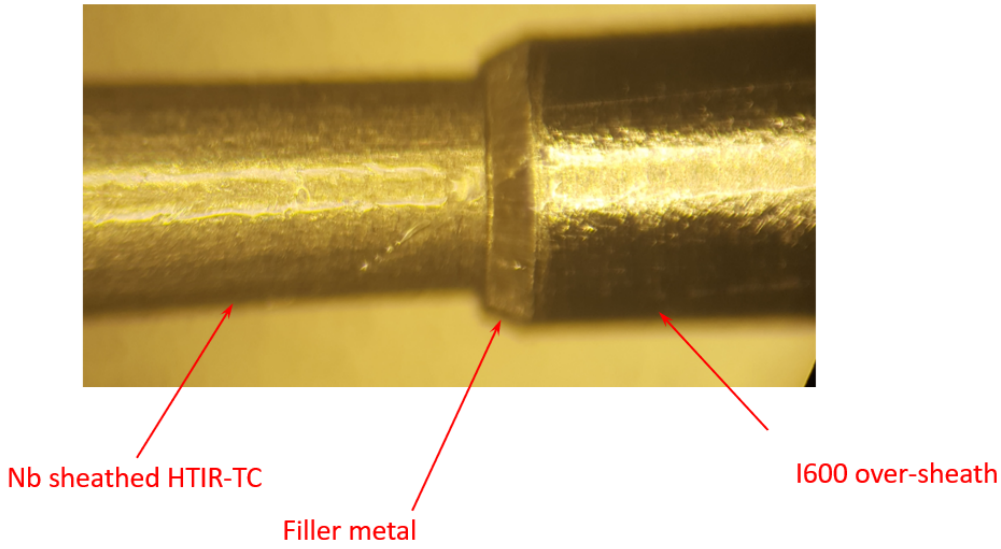

Figure 19. I600 welded to Nb sheathe HTIR-TC.

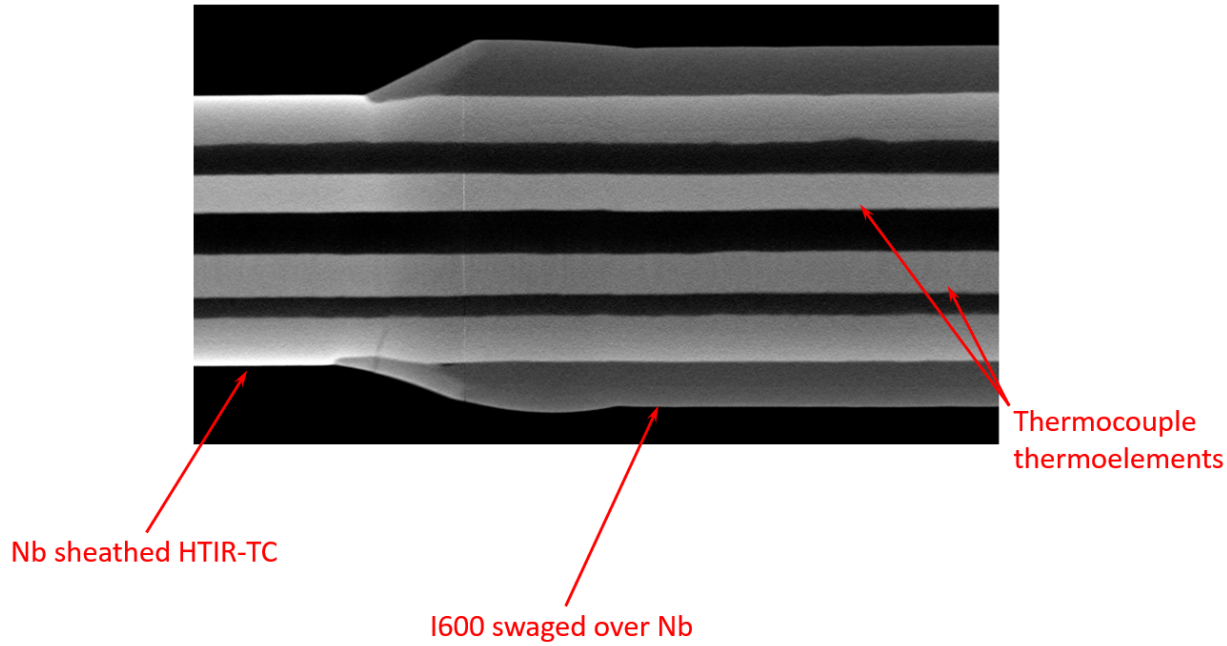

Figure 20. CT scan of I600 over-sheath welded to Nb HTIR-TC.

A variety of tests were conducted on the dual walled thermocouple. In the first test, an I600 tube was placed loosely around a HTIR-TC, and the weld shown in Figure 17 was made. Then a vacuum was pulled on the far end of the I600 tube while the weld area was flooded with He. No leakage greater than 1.0 E-06 std cc/sec was observed[b].

[b] IFE engineers stated that they've obtained similar leak-tight results when making welds between the equally incompatible combination of Zr to I600. They stated that these "welds" ("bonds" might be a more appropriate term) are typically leak tight but very brittle and subject to fracture if any significant mechanical loads are applied.

In the second test, an I600 tube was swaged tightly over an HTIR-TC, but no weld was made between the tube and HTIR-TC sheath. Again, the area where the weld would have been was flooded with He while a vacuum was pulled on the far end of the I600 tube. No leakage greater than 1.0 E-06 std cc/sec was observed.

The final test was on the sealing ability of the potting epoxy in the transition cup. A metallic transition cup was brazed to an I600 tube and filled with epoxy (Re. Figure 14). Helium was applied to the open end of the I600 tube while a vacuum was pulled from the top of the transition cup. No leakage greater than 1.0 E-06 std cc/sec was observed.

These tests provide a measure of confidence that the arrangement shown in Figure 14 is capable of preventing fission product release into the space above the ATR top head closure plate. However, additional testing is required to fully validate the arrangement. The first two tests need to be repeated at a temperature corresponding to loop water temperature (i.e., approximately 300°C). Because I600 has a higher coefficient of thermal expansion than Nb, the assemblies may not seal as well if the temperature is elevated.

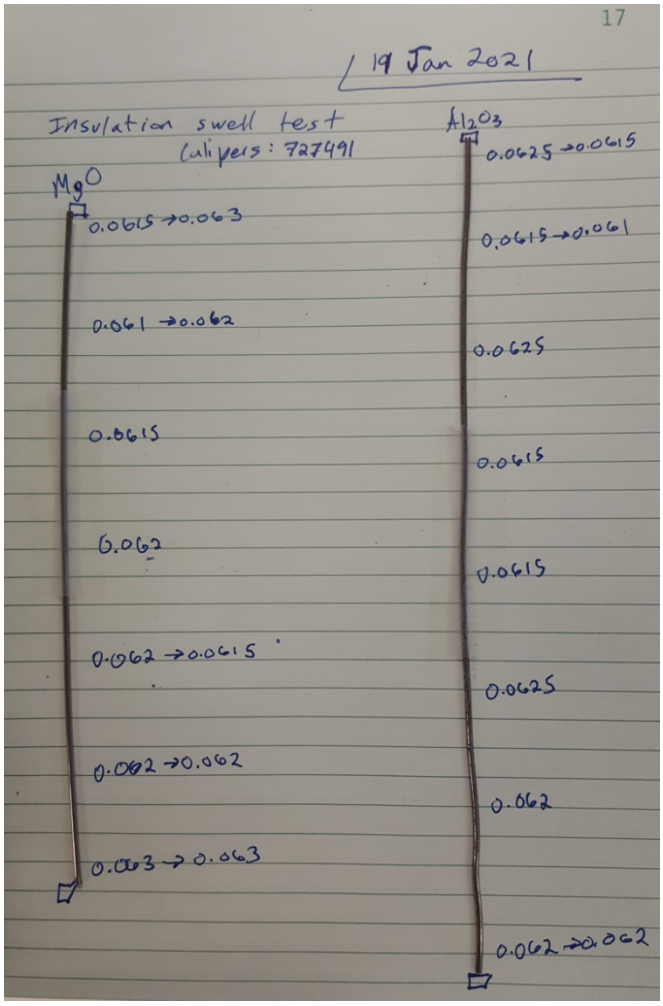

Figure 21. Results of swelling test on mineral insulated cable exposed to water at pressurized-water reactor (PWR) conditions. Where measurements are in pairs, the left side measurement was made before placement in the autoclave, and the right side was made after the autoclave test.

This test on the epoxy showed the epoxy to be leak tight but did not demonstrate that it could hold against full loop pressure or against the maximum postulated fission product gas pressure (because of the location, this epoxy does not experience loop temperature). IFE engineers have provided guidance on measures that can be taken to strengthen the epoxy's grip on the transition cup, so that it can withstand forces from high-pressure fluid (either fission product gases or loop water), and the testing of this upgraded design may be an appropriate activity for FY-22.

One further related test was performed. This test arose from the scenario that, in the event of a breach of the rodlet pressure boundary, water could perhaps enter the TC cable. Hearsay suggests that MgO insulation, being hydrophilic, can absorb water, swell, and essentially "unzip" the sheath all the way up to the seal at the reactor top head. It's been proposed that this unzipping could be so severe as to allow loop water to escape into the space above the ATR top head closure plate. As an initial effort to investigate the plausibility of this scenario, two lengths of 1/16-in.-diameter mineral insulated cable, with both ends open, were placed in an autoclave at PWR conditions for 24 hours. The results from this test were that neither cable showed any signs of "unzipping" or even swelling over this period of time (Figure 19). At a minimum, this demonstrated that the phenomenon proposed is very slow to develop. Further testing of this scenario may be warranted in FY-22.

Notable features of the arrangement designed by INL hot cell engineers (see Figure 20) are as follows:

- This initial design is for fresh fuel and fresh cladding, thus most of the complications of the IFE design are not pertinent here.
- Similar to the measurement sciences design, a Conax fitting with a grafoil sealant is used to seal around the thermocouple cable. In this case, the thermocouple is assumed to be a standard Type K, I600 single sheath, 0.062-in.-diameter design. Nothing in this design would preclude the use of high-temperature-capable thermocouples, such as the dual sheathed HTIR-TC described above.
- This design features two circumferential welds (labeled in Figure 20 as "TIG WELD") and a final weld on the 0.020-in.-deep hole shown in Detail A. Unlike the IFE scheme, which fully encloses the rodlet in an inert chamber, this weld procedure simply shrouds the circumferential weld zones and floods the shroud with argon. This method has been proven to produce sound, ductile welds. The final weld, which seals up the weep hole, is made using the Weld Under Pressure System (WUPS). The WUPS seals around the cladding outer diameter (OD) just to the right of the weep hole nipple. The WUPS, as its name suggests, is capable of pressuring the rodlet (with an inert gas composition of the user's choice) and then sealing off the weep hole.
- It is expected that some variation of this design could be used for re-instrumenting previously irradiated rodlets. One notable issue to be addressed is that there is no weep hole above the fuel stack. This risks blowing out the right side circumferential weld if there is no gas path through the irradiated fuel stack. IFE engineers have stated that there is frequently a gas path through the irradiated fuel. Furthermore, other capsule designs at INL have avoided the need for a weep hole by using well-designed copper heat sinks adjacent to the weld zone.

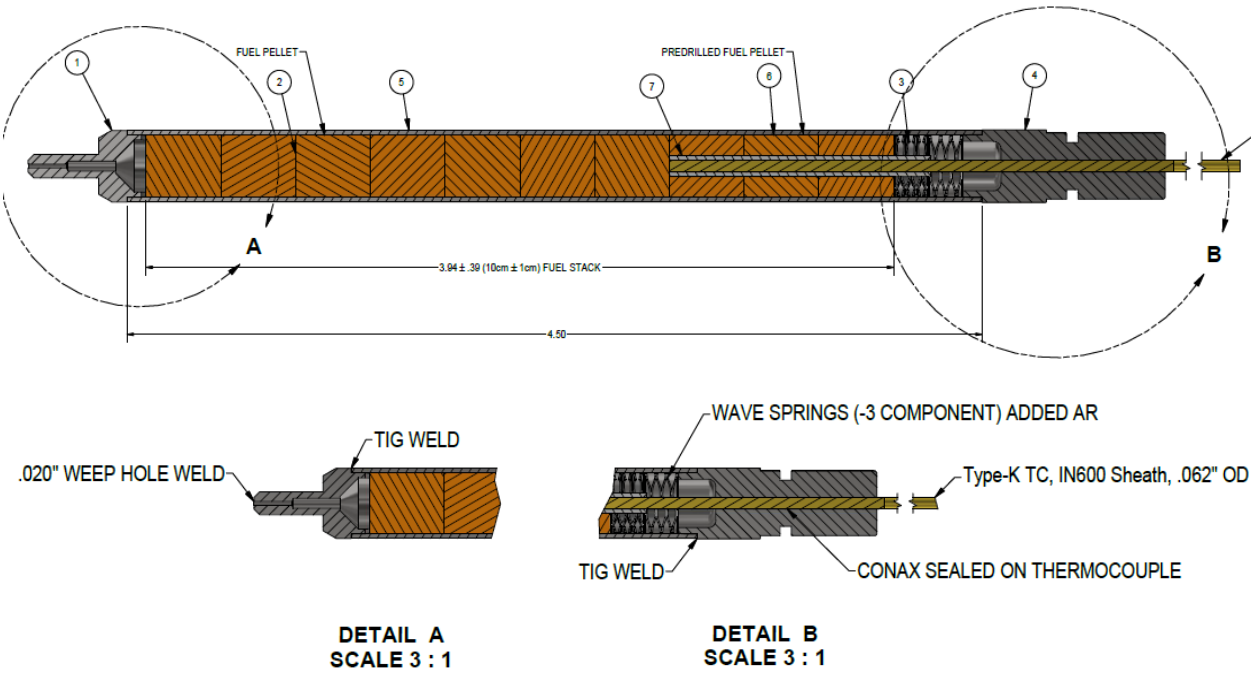

Figure 22. Fuel pin design by INL hot cell engineers.

5. Instrumented Fresh Fuel Rodlet Assembly

A fully-assembled fuel rodlet containing a fuel centerline thermocouple was fabricated as a culmination of several efforts detailed in previous sections of this report. The successful assembly of this rodlet specimen relied upon drilling techniques suitable for creating an annulus within ceramic fuel pellets. It also necessitated a rodlet endplug capable of accommodating a thermocouple as fed through the endplug and into the fuel within the rodlet. This endplug is a custom-manufactured Conax component made from Zircaloy-4 as a compatible material with rodlet cladding and also with a grafoil seal specifically manufactured to mate with the 0.063-in.-diameter thermocouple. Figure 21 contains a cross-sectional representation of a fuel rodlet with centerline thermocouple. The custom Conax fitting is exhibited on the right-most part of the rodlet and also as Figure 22.

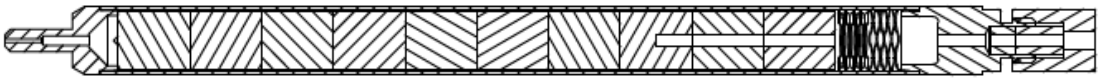

Figure 23. Cross-sectional representation of a fuel rodlet capable of accommodating a thermocouple within the upper fuel pellets.

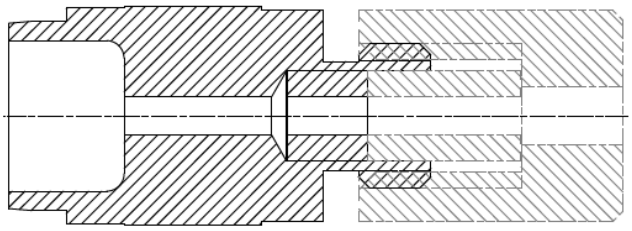

Figure 24. Enlarged representation of a custom Conax fitting suitable of thermocouple installation within a fuel rodlet. The left end contains a weld joint to mate with the cladding tube.

The general assembly sequence of this rodlet begins with welding a bottom endplug using standard rodlet assembly techniques, followed by the fuel loading of the non-drilled pellets into this partial assembly. One objective of the rodlet assembly was to demonstrate an extremely small radial gap between pellet annulus and the centerline thermocouple. As a result of minimizing this gap, the drilled fuel pellets had to be loaded onto the thermocouple prior to final assembly within the rodlet and mechanical pressing of the top endplug into the cladding. Prior to this pellet loading step, the thermocouple is fed through the Conax, and the Conax is torqued such that it forms a seal around the thermocouple. Figure 23 shows these two partial assemblies prior to final mechanical pressing of the Conax endplug to the rodlet cladding tube. This joint is then welded via laser welding.

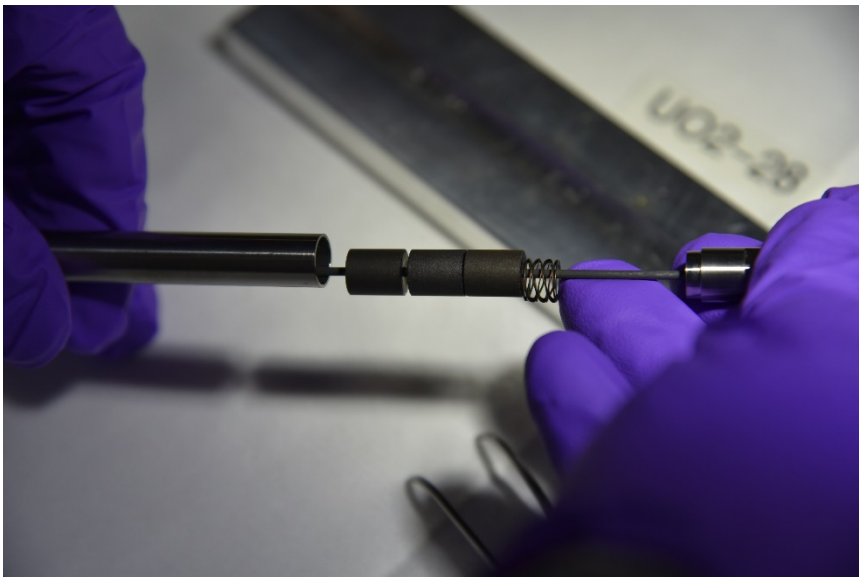

Figure 25. Assembly of a rodlet containing a fuel centerline thermocouple, including a custom-manufactured Conax plug through which the thermocouple is fed. Fuel pellets containing an annulus are visible as loaded onto the thermocouple.

The final seal welding of the rodlet is accomplished using the WUPS, which was designed and built at INL to evacuate, refill, pressurize, and seal-weld specimens via a small diameter weep hole in the rodlet bottom endplug. A radiographic image of two instrumented rodlet assemblies is shown in Figure 24. All rodlet constituents are readily visible within the radiographic image; however, the thermocouples are not visible within the fuel pellets themselves. This represents an inherent limitation to x-ray radiography as a result of the x-ray absorption of the uranium-bearing fuel pellets, hindering the ability to resolve the drilled hole within the pellets or the thermocouple location within the fuel pellet centerline.

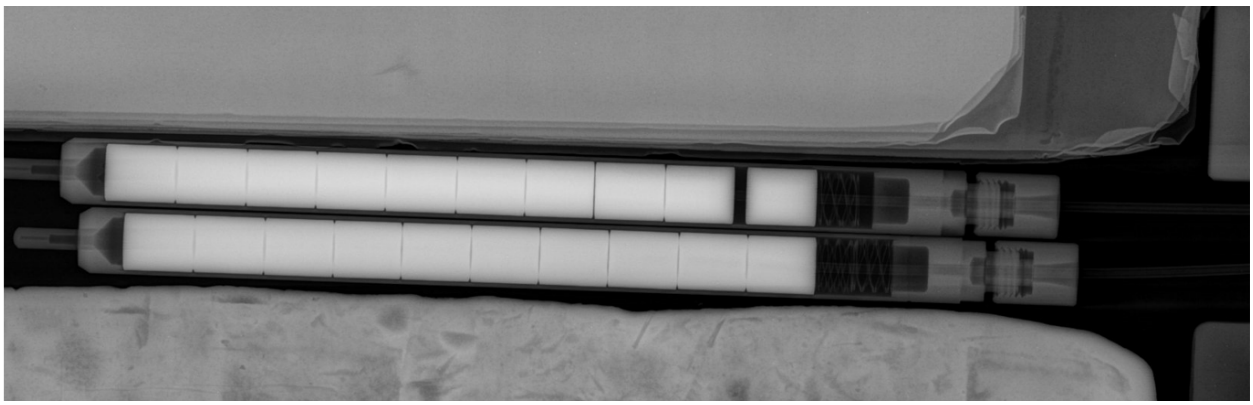

Figure 26. Radiographic images of instrumented fuel rodlets. The thermocouples are visible through the top endplugs towards the right of the radiographs while the fuel pellets are clearly identified as the white cylindrical objects.

In the case of these specific rodlets, laser welding for the top endplug is the most suitable sealing method to minimize heat input, which could negatively affect thermocouple performance or the performance of the grafoil seal within the Conax endplug. Traditional TIG welding techniques require significantly higher heat inputs, which may not be compatible with the assembly sequence.

It's important to note that this evolution focused on assembling a fresh fuel rodlet with a centerline thermocouple that is within 0.001 in. of the fuel pellets themselves. There are multiple applications for instrumented fuel rodlets, including those where a much larger distance between thermocouple and fuel pellet is acceptable. In these instances, the assembly sequence would likely be varied to weld the top endplug into place before the installation of the thermocouple itself or the seals around the thermocouple, thus negating the need to consider damaging these as a function of welding heat input.

6. Surface Thermocouple Modeling

Colby Jensen and Kevin Terrill

6.1 Introduction

Measuring surface temperature is challenging in any environment, but for a surface immersed in water, very few options are available. One of the best and most common strategies relies on a bare wire thermocouple (TC) welded to the surface to form an "integral" junction through the surface (if metallic) itself. Still, the presence of the TC wires impacts the measured parameter by creating additional heat transfer to the coolant through a fin effect and altering local 2-phase heat transfer behavior. Previous studies have shown that there is a significant difference between the surface temperature where the wires are welded to the surfaces [1,2,3,4]. The use of integral junction thermocouples has been proven effective for the high response times needed for transient testing.

6.2 Problem Description

The purpose of this work is to characterize and quantify the bias errors from different types of thermocouples and their attachment methods to the cladding surface. The thermocouples are in an integral junction configuration with the wires welded to the cladding surface where the surface is a part of the hot junction. To develop a correction factor for the measured data of the TC, a range of thermocouple parameters are investigated to understand their direct impact on the heat transfer error. The variables investigated are the thermocouples' weld energies, thermoelement wire size, wire separation, and attachment method. A range of heat transfer scenarios were investigated, ranging from cladding-to-water and cladding-to-film heat transfer.

The modeling done is based on the Type R thermocouple due to their rated use in the high-temperature range required for transient tests and their compatibility with Zr-based claddings. The thermocouples are recommended for measuring temperatures from -50 to 1480°C. The material compositions of Type R thermocouples are 87% platinum and 13% rhodium for one thermoelement and 100% platinum for the other. These materials allow for a high accuracy and stable reading at extreme temperatures due to the higher composition of rhodium, with a reported accuracy of 1.5°C or 0.25% of the reading during stable steady-state conditions.

The thermocouple wire diameter is selected to minimize its impact on measurement while being large enough to facilitate practical installation and handling. Two different diameters of thermoelements are investigated with an individual wire having a diameter of 0.005 in. and 0.01 in. This study will assume the following conditions:

- Coolant: Stagnant water at atmospheric conditions
- Measured surface: Zirconium cladding without oxidation
- Thermocouple: 13% - rhodium 87% - platinum / platinum.

The variables investigated in the bare wire thermocouples include the follow parameters: the weld energies used to attach the thermoelements. The placement of the thermoelements included orientation, spacing, and thermoelement diameter. The change in heat transfer is due to fin effects when the rod interacts between either water, steam vapor or a combination of the two.

Standardizing the method of attaching bare wire thermocouples allows for the ability to quantify the error associated and to develop correction factors. The fin effect is investigated under the specified parameters described above. The modeling was done in COMSOL to determine the fin effect of different placement and attachment methods of thermoelement leads. The investigation of the heat transfer will determine optimal placement of the thermoelement leads to minimize the fin effect. Figure 25 shows the baseline model used to calculate the different attachments based on early experimental wire attachment trials shown later. The standard model uses two-dimensional layout that has a small film layer and a larger water layer around the heater rod as seen in Figure 25. The primary attachment method investigated is the parallel attachment method

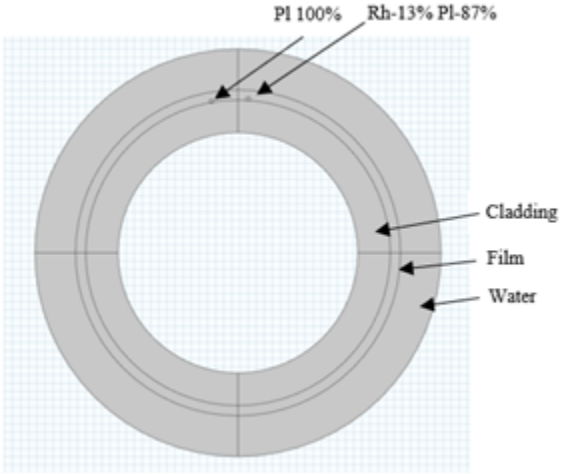

Figure 27. 2D COMSOL model of the thermocouple attachment.

The model's boundary conditions are placed to focus on the heat transfer between cladding, coolant, and the thermoelement. The inner diameter of the rod is thermally insulated. The thickness of water is large enough to provide a bulk temperature. The model assumes limited flow in the liquid sections of the model. The liquid velocity is set to zero to simulate conduction heat transfer to use a conservative

approach. The current model design takes a simplified approach to a nuclear fuel rod to eliminate the gap conduction problem between the fuel rod and cladding surface. A boundary heat source is placed on the inside diameter of the cladding to represent the heat from the fuel. The model is further simplified by removing any secondary heat source in the cladding that may occur during actual reactor conditions. Lastly, the model obviously does not include the impact of the lead wire that would extend away from one end of the attached region, which may impact estimates of heat loss in that region. The 3D model better addresses these effects.

COMSOL is a 3D multiphysics tool that is designed to look at the heat transfer relationships between different geometries and material properties. Most of the modeling was done in this study with the 2D geometric layout, but since COMSOL is a 3D modeling tool for the heat transfer, the depth can be controlled. The default depth is set at 1 m, but for these studies, the depth was changed to a ¼-in. depth. The maximum length of the parallel orientation attachment was changed to be a ¼ in. This depth prevents the assumption of an infinite fin but rather takes a snapshot of the local area where the fin is placed in the cladding surface. Localizing the fin z location allows for the actual fin surface area to be used in the model. The z boundary is isothermal at the end points, but the location of the TC attachment location and the ends is significant to minimize any isothermal boundary conditions.

An additional model layout was used to model the 3D space for the heater rod. This model will test the different attachment methods. Both methods have distinct advantages for attachment welding theory. This model will determine the heat transfer effect that the long leads have on the parallel attachment method. Figure 26 shows the 3D attachment model used to determine the heat transfer and fin effect.

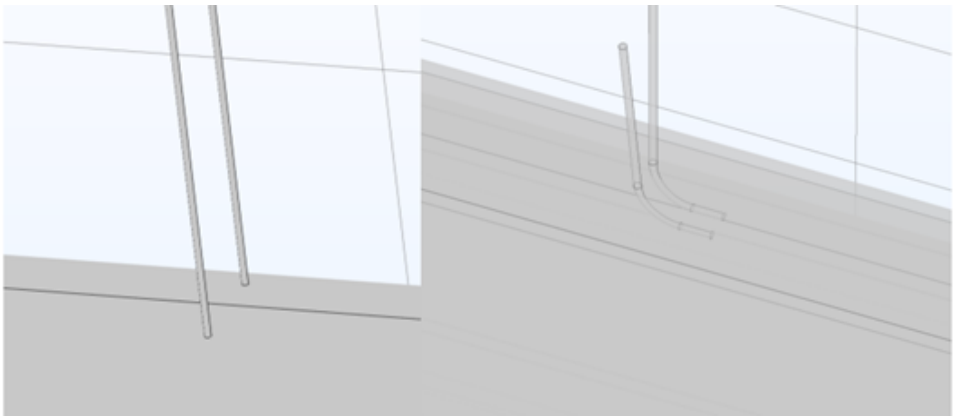

Figure 28. The different thermocouple welding attachment methods modeled in COMSOL. The left side is the perpendicular orientation, and the right side is the parallel attachment method.

The mesh used on the model was based on the area of interest and the heat transfer physics used in the COMSOL model. The thermoelement leads contain a higher portion of mesh around the area to provide a more accurate temperature layer throughout the area. This mesh orientation will allow a different temperature distribution through the film, the thermoelement cross section, and the water around the area. A fine mesh is used around the thermoelement leads for increased detail of their performance in both the 2D and 3D models seen in Figure 27 and Figure 28. The temperature is taken at the area where the thermoelement lead is attached to the surface area of the thermoelement lead. An average temperature along the surface connect area is taken to be compared to the surface area.

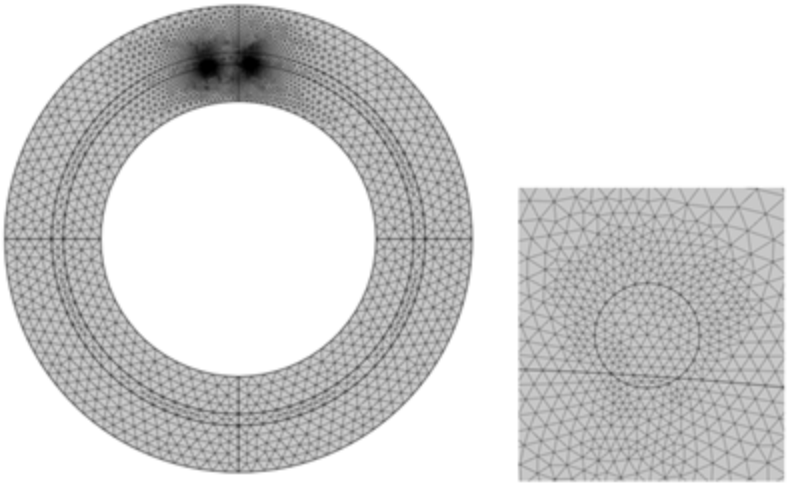

Figure 29. Mesh for the 2D model used for the parallel attachment method. The mesh is at a higher density around the thermoelement areas to help determine the temperature profiles around the fin area.

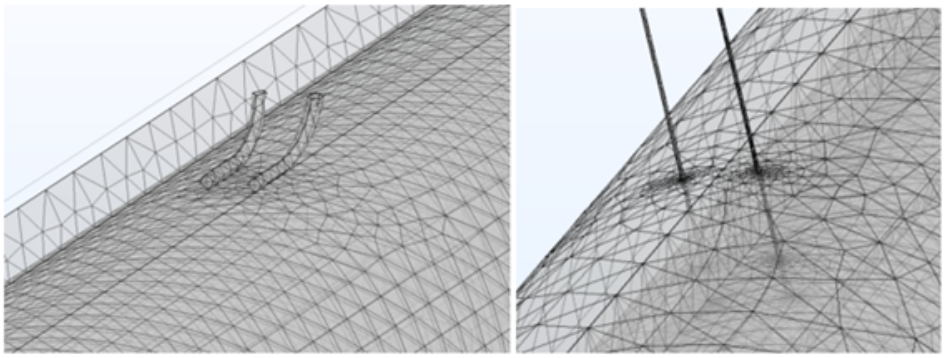

Figure 30. Fine mesh used for the 3D COMSOL model. The two areas of highly refined mesh are for the thermoelement leads at the surface attachment and when the leads cross over between the film and water coolant area.

All variations of the model used the same mesh parameters and initial conditions. The main difference is the change of weld energies (described next), thermoelement spacing, thermoelement diameter size, and attachment orientation method. The assumptions to the model are that all tests are done in pool water conditions and do not have an active flow across them. The thermoelement leads are attached directly to the surface of the cladding, and the average area between the two leads is compared to a similar area on another section of the cladding.

There is a baseline model used to compare the different parameters to determine how the surface temperatures are affected. First wire attachment studies focused on laser welding wires to zirconium surfaces. The results of those trials are used here to explore the potential impacts of resulting configurations. The standard option modeled are set as follows; 1-mm spacing between thermoelement leads, 0.7 J welding energy, 1 mm of film thickness, and set material properties for Zircaloy 4 and Type R thermocouples. Table 2 details all the parameters used in the COMSOL model. Only two thermoelement diameters were used for the study, 0.005 in. and 0.01 in. Although different diameters exists for Type R thermocouples, the typical diameters used in current operation are between 0.005 and 0.01-in.

Table 2. The COMSOL model dimension and material properties used in the COMSOL Model.

Fuel Rod PWR		
Cladding		
ID		
OD	9.5	mm
Wall Thickness	0.572	mm
Material	Zircaloy-4	
Density	4,800	kg/m^3
Thermal Conductivity	13	w/mc @400°C
Heat Capacitance	330	J/kgc @400°C
Thermocouple		
Type	R	
OD	0.01 0.005	in.
Spacing	1 to 3	mm
Material Thermoelement 1	platinum (Pt)	
Density Pt	20,000	kg/m^3
Thermal Conductivity Pt	71.6	w/mc @400C
Heat Capacitance Pt	125	J/kgc @400c
Material Thermoelement 2	platinum 87% rhodium 13%	
Density Pt87Rh13	19,600	kg/m^3
Thermal Conductivity Pt87Rh13	60	w/mc @400C
Heat Capacitance Pt87Rh13	135	J/kgc @400c

The welding energy determines the cross section of the leads to the surface as shown in a study done from Boise State University with the Idaho National Laboratory University.[5] Figure 29 shows how different welding energies may affect the cross section of the thermoelement leads and the depth into the cladding surface. A major consideration for using the weld energies is the depth penetration into the surface. This consideration will factor into the focus of the parametric study done in COMSOL.

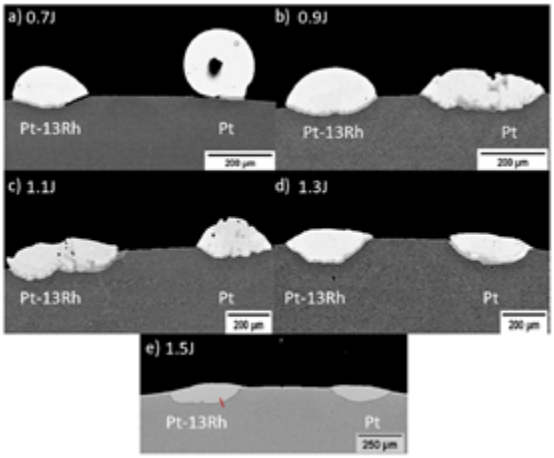

Figure 31. The cross section of the two thermoelements welded to the Zr cladding at different weld energies. Study done by Boise State University.

The weld energy determines the depth penetrations of the thermoelement into the cladding. The high energies will deform and reshape the thermoelement, creating different fin effects. The different welding energies are represented in Figure 28 and how the COMSOL model changed the TC cross section based on the different weld energies.

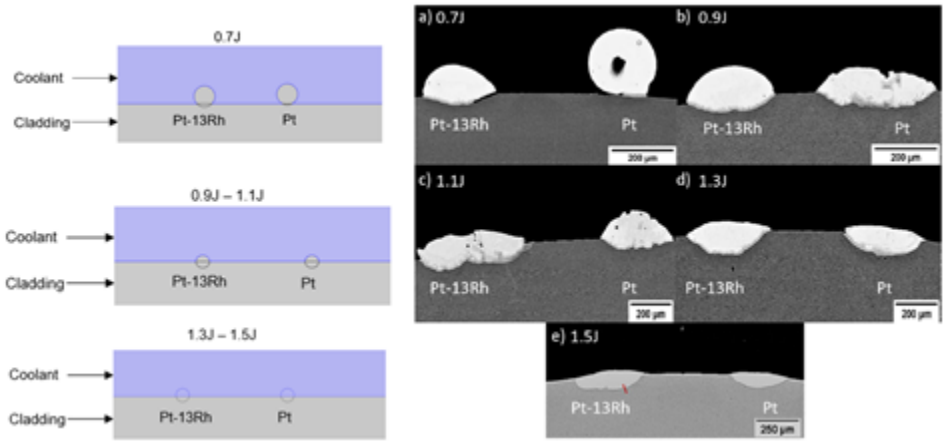

Figure 32. The COMSOL representation of the cross-section thermocouples attachment at different weld energies. The different weld energies are combined into three different groups for simplicity. The low energy is considering a surface attachment where there is minimal penetration to the surface of the cladding.

A consideration between the penetration depth and the fin effect will determine the error associated with the TC performance. The connection point between the thermoelement and cladding is investigated through investigating different depths. The separate models were used to investigate the temperature reading between the two points based on depth.

A major consideration with thermocouple welding is the depth into the cladding surface. Increased welding depth raises the risk of causing a weak spot on the cladding surface that can cause unwanted breakage or failure. Increasing the weld energy and the penetration depth on a standard cladding thickness may have a significant impact on the remaining thickness . Table 3 gives the relationship between depth of the weld to the percentage of the cladding that remains after the penetration is made.

Table 3. Depth penetration from weld energies into the cladding surfaces.

Indentation of the Thermocouple on Cladding				
TC Diameter (mm)	0.254		0.127	
Cladding Thickness (mm)	0.572			
Max Depth (mm)	0.445	78%	0.509	89%
Half Depth (mm)	0.509	89%	0.54	94%
Small Depth (mm)	0.53	93%	0.551	96%
Surface Depth (mm)	0.547	96%	0.559	98%

The initial setup of the modeling allows for small adaptions to be made to run the parametric studies needed to determine the fin effect caused from the thermocouples.

6.3 Results and Discussion

The initial investigation on the temperature difference between the measured surface subject to the fin effect and an untouched surface on the rod for a range a situation. The design of the modeling is to find trends on the different attachment methods to understand how the measured temperature is affected. This study will assist in the decision-making on how to standardize thermocouple attachment methods used for

TREAT experiments. The initial investigation is on weld energies and how thermoelement depth affects the measured temperature. The weld energies were grouped into three different weld energies shown in Figure 28. The modeling used a standard 2D model described above, and the model was investigated at two different thermoelement diameter size. Table 4 shows the modeled data comparison between the different weld energies.

Table 4. Temperature difference between surface temperature and thermoelement for a range of welding energies and depth penetration.

Temperature Difference on Welding Energies at 1400 K		
Welding Energy (J)	0.01-in. Diameter	0.005-in. Diameter
0.7	140.2	35.6
0.9–1.1	80.4	32.5
1.3–1.5	-7.7	-6.3

As the depth of the thermoelement increases, the less fin effect is seen from the models. Due to the attachment assumption, the study will only present the attachment used with the 0.7 J welding indentation until a standard has been set. The different attachment parameters will be investigated with the 0.7 J welding energies for two different thermoelement sizes of 0.01-in. and 0.005-in. diameters. A standard model was used to determine how the thermoelement sizing has on the fin effect and the temperature difference. The larger thermoelement diameter will cause an increased fin effect due to the increased surface area. The negative temperature shows that the weld area has an increased temperature reading to that of the surface temperature. This is thought to be from the increased depth the thermoelement lead has in the cladding. The average temperature between leads is higher than the surface.

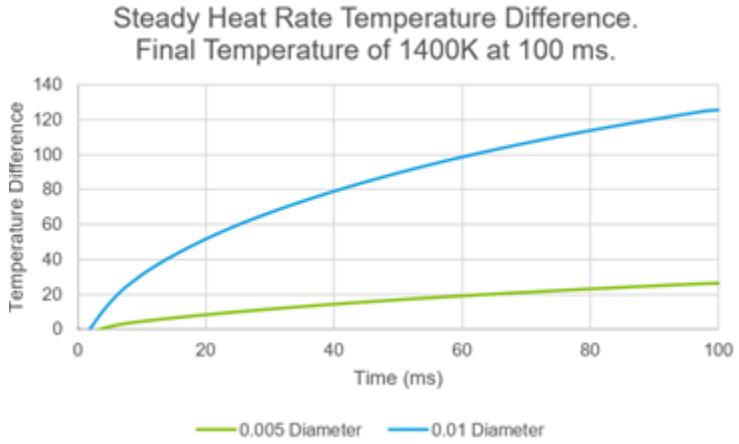

Figure 33. The temperature difference for the area around the thermoelement leads and the surface temperature. The larger diameter as expected, has a significant temperature difference. The fin effect is only analyzed on the 2D model.

This will provide the range of error anticipated from the fin effect with the potential thermoelement sizes. The larger the diameter, the greater the temperature difference as shown in Figure 31. The rest of the modeling for the different parameters will be done with both thermoelements to determine the fin effect. Uncertainty remains on how the thermoelement leads leaving the surface of the cladding affects the fin effect. The larger diameter thermoelement leads could have a higher fin effect with modeling the leads extending from the surface of the cladding.

The initial studies investigation of the actual temperature were modeled between the thermoelements and the surface temperature of the same rod. The initial study investigates the spacing of the leads at 1, 2, and 3 mm. The model results show this is a minimal fin effect from the spacing of the thermoelements. This does not account for the voltage reading that the thermocouple would be subjected with increased

spacing.

Table 5. Temperature difference between surface temperature and thermoelement as the leads are separated by 1–3 mm. As the leads are placed closer, there is a greater fin effect.

Temperature Difference on Spacing Between Leads		
Spacing (mm)	0.01-in. Diameter	0.005-in. Diameter
1	153.5271292	39.7907828
2	123.5891267	32.37287712
3	100.4702696	27.7906905

The spacing between the two thermoelement leads was investigated to determine the fin effect between the surface temperature and the thermoelement leads. The two different thermoelements diameters were modeled to show the temperature difference and to investigate the potential fin effect.

The smaller the fin is, the lower the expected temperature difference. A determining factor is the heat transfer through different film thickness layers and investigating how the heat transfer is affected when the fin is partially covered with water. Figure 32 shows how the film thickness effects the temperature difference from the thermocouple and the surface. The zone of 1 mm–2 mm is established as the typical film thickness expected from transient pool boiling experiments.

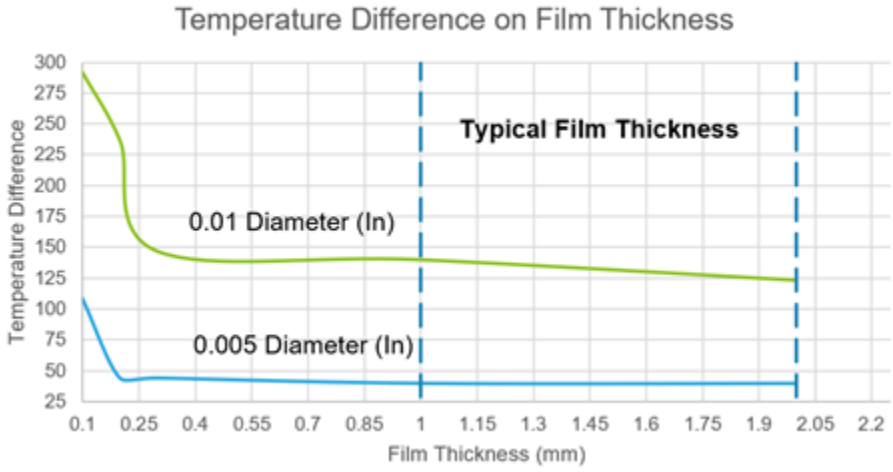

Figure 34. The temperature difference at different film thickness around the rod.

As flow boiling transient experiments are investigated in the future, the typical film thickness will fall between 0.5 and 1.5 mm. The partially covered thermoelement causes a significant temperature difference and a large uncertainty in the temperature differences.

The challenge of determining the film thickness for transient boiling is the oscillation viewed during transient testing. During the transient testing done in both out-of-pile and in-pile facilities, film oscillation has been witnessed and investigated. The oscillation has a spacing of 1–3 mm between peaks and frequencies from 333 to 1,000 hz. [1] This phenomenon happens during film boiling during experiments, but an average film thickness is determined at the amplitude of the oscillation.

A major concern is that the thermoelement leads are still be covered with water and the surface be covered in film or a single lead is covered in water and the other in film due to oscillation. Results from the transient pulse power facility at the INL shows that this is a potential problem. During testing on a heater rod, a high-speed camera on the thermoelement leads showed that the welded area creates a pocket of water where the thermoelement leads are fully covered in water and the surface of the rod remain in film. This also disturbs the film flow across the cladding surface.

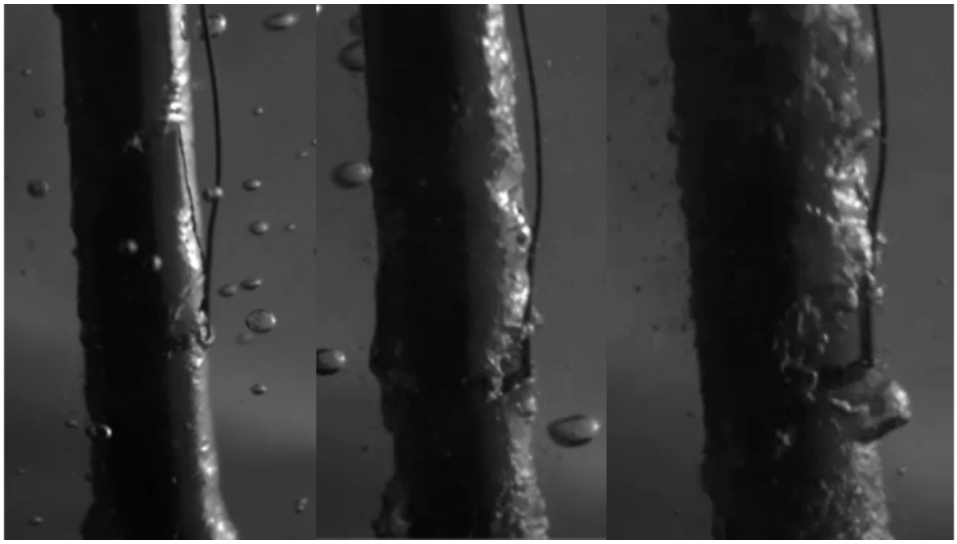

Figure 35. Images taken from a video focused on a thermocouple attachment. The conditions of the test were at 10 degrees subcooling with a 100 ms power pulse. The image on the left is at 150 ms. The center picture is at 700 ms. The picture on the right is over 1,000 ms.

The thermocouple has a cooling effect on the localized area of the cladding surface. The disruption of film flow across the thermocouple area is an area of uncertainty that has a major impact on the temperature output. To model this situation, the extreme conditions were modeled where a single lead is covered in water and the other covered in film for the duration of the power pulse. To simulate the oscillation, a model was adjusted to show the difference between the two leads.

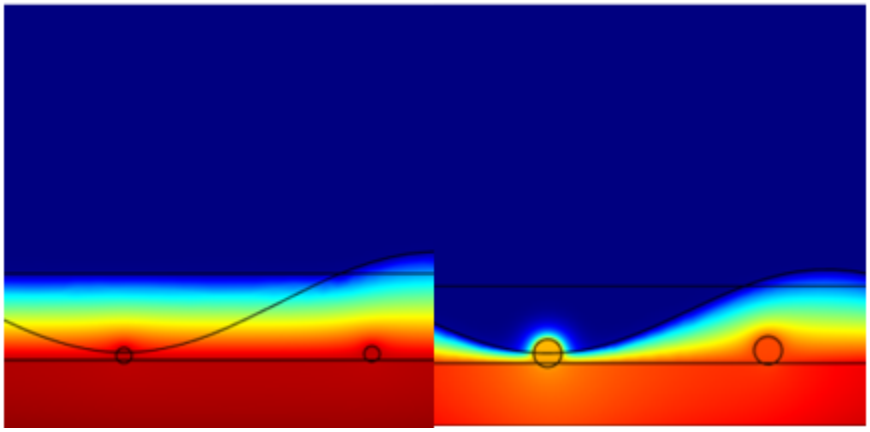

Figure 36. Left: 0.005-in.-diameter thermoelement leads. Right: 0.01-in.-diameter thermoelement leads.

Instead of taking the average temperature between leads, the average temperature of each lead is specified in Table 5. The voltage generated during these conditions will need to be further investigated. There is a significant temperature difference between leads for the larger diameter thermoelement lead.

Table 6. Oscillation temperature difference between the two leads. The temperature difference is between the thermoelement leads. The uncertainty of the voltage generated in this situation is a large uncertainty.

	Large Connection				Small Connection			
Power Level	Surface Temp.	Lead 1 Temp.	Lead 2 Temp.	Temp. Difference	Surface Temp.	Lead 1 Temp.	Lead 2 Temp.	Temp. Difference
High	513.01	458	480.4	22.4	516.29	509.63	510.24	0.61

Power								
Medium Power	732.32	625	667.1	42.1	738.88	726.42	728.3	1.88
Low Power	1390.3	1114.7	1226.8	112.1	1405.3	1372	1375	3

The last consideration is the orientation of the leads to the surface of the cladding. There are two proposed welding orientation onto the cladding surface; a perpendicular attachment and a parallel attachment scheme.

The different orientations were modeled to determine the effect each method would have on the heat transfer fin effect. The parallel scheme has a larger area affected by the fin effect due to the longer length, as shown in Table 7. The temperature was taken at the surface depth of the thermoelement and at the center location of the length along the thermoelement leads and cladding. The area to measure remains an uncertainty for the parallel case due to the size of the area measured.

Table 7. The temperature difference due to the attachment orientation. The results shown on the table is for the 0.01-in.-diameter thermoelement leads.

	Parallel Connection			Direct Connection		
Power Level	Surface Temperature	Temperature TC	Temperature Difference	Surface Temperature	Temperature TC	Temperature Difference
High Power	1660	1520	140	1660	1600	60
Medium Power	1000	910	90	1100	1050	50
Low Power	640	600	40	650	610	40

The larger area contributes to the active removal of heat during the transient tests at higher powers. This signifies that the larger fins' surface area contributes to more heat removal and a larger temperature drop.

6.4 **Modeling Conclusions**

Several models were developed to investigate the bias error caused by thermocouples welded to surfaces in boiling-water conditions. First analyses are focused on trial welding approaches developed to date that characterized the junction area geometry. As expected, these analyses show a significant impact on the heat transfer between the surface of the test rod and the surface where the thermoelement leads are welded. The different parameters investigated will help determine the standardized attachment method to be used in future experiments. From the parametric study done, the largest contributions on an increased temperature difference is weld energies, orientations, and thermoelement spacing. The film thickness effect was analyzed to show the range of bias introduced, shown to be important for these types of measurements. A final decision on the attachment process and resultant junction configuration will allow for the development of a specific correction factor. These analyses will support attachment development and eventually be crucial for accurate measurement interpretation.

Two different thermoelement sizes were investigated with the expectation that the thermoelement to be used will be between 0.005 and 0.01 in. in diameter. Clearly, a smaller diameter wire provides a better performance but that will need to be balanced with weldability and handling requirements. The welds must be able to maintain their integrity during all handling and transportation and during a test, but the

smaller diameter will minimalize the fin effect. The preferred wire size is 0.005 in. to achieve these ends—though continued experimental development may indicate the need for a slightly larger wire size. For integral junctions to work accurately, the individual junctions of the two thermoelements with the surface must be assumed to be isothermal. Future work may also consider the impact of violating this assumption from the standpoint of calculating additional voltage generation between the junctions and associated impact on output temperature.

Further work will look at different thermocouple junctions to determine the temperature drop. Sheathed thermocouples welded to a surface are also planned to be used in some experiments in TREAT. Sheathed thermocouples should provide more robust performance but are not well suited for fast transient conditions due to the thermal inertia associated with their geometry. However, experiments, such as loss-of-cooling accident testing, have much longer time constants associated with surface temperature events to allow for their use. Therefore, in addition to supporting integral junction bare wire thermocouple methods, sheathed thermocouple attachment configurations will also need to be analyzed in the future to assess their impacts. Future work will also need to address flow boiling

7. EPIC Hot Cell Development

Basic refabrication equipment has been successfully installed and demonstrated in INL's large hot cell, HFEF. Despite this, the anticipation of more advanced re-instrumentation needs and larger/longer fuel segments supports the need for a dedicated shielded facility to perform this work in. Two significant accomplishments this year have been completed and include a first phase capability development plan for the TREAT Experiment Support Building (see PLN-6301), which in the near term can support the assembly and checkout of highly instrumented fresh fuel experiments. The second accomplishment is the conceptual design of the Experiment Preparation and Inspection Cell (EPIC), which is a shielded enclosure and can support the refabrication and advanced re-instrumentation activities on irradiated fuel segments up to 4 ft in length (see TEV-4341). These plans are significant as they support the strategic readiness to execute detailed design activities, fabrication, and installation of equipment, should funding become available.

For additional details, the reader is referred to PLN-6301: Capability Development Plan for TREAT Experiment Support Building, and TEV-4341: Conceptual Summary of EPIC System.

8. Conclusions

The loss of the Halden Reactor, and the associated knowledge and capabilities, continues to be impactful to the nuclear fuel research community. Thanks to early action and intervention, basic capabilities to refabricate fuel segments and assemble them into follow-on experimental conditions for either in-pile or out-of-pile testing is now available. As noted at the beginning of this report, Halden continued to refine and advance their refabrication and re-instrumentation capability for nearly 30 years. Embarking on this path, INL successfully developed the capability to drill centerline holes in fresh UO_2 fuel pellets to support the assembly of advanced instrumented fresh fuel rodlets for irradiation testing. INL also successfully developed a first-generation end fitting for rodlets to support fuel centerline instrumentation leads. It is anticipated that this new capability will be put to use for an instrumented rodlet test to be irradiated in FY-22.

In anticipation of developing irradiated fuel drilling capabilities using the existing HFEF Mini-Mill, fuel drilling parameters were developed that account for the limited spindle speeds capable on the HFEF Mini-Mill. It is expected that drilling centerline holes in irradiated fuel using the HFEF Mini-Mill will continue development in FY-22. Concurrently, INL pursued a technology transfer approach and obtained both a fuel drilling and fuel segment welding system from Halden. These systems were assembled, and initial evaluations were performed. Having these systems in hand also supported conceptual design activities for the EPIC hot cell in establishing space allocation and utility requirements. Non-fuel surrogate testing using the Halden provided systems will be performed in FY-22 and will support future

design decisions for the deployment of an advanced refabrication and re-instrumentation system.

A further collaboration and technology transfer with Halden provided insight into the complex advanced refabrication and re-instrumentation process being used by Halden. This review made clear that many more welds are required to complete the full assembly of a rodlet with advanced instrumentation than the three welds currently possible on the INL basic refabrication system. This review also illuminated the complex sealing methods Halden used to mitigate gas leaks in the refabricated rodlets. In FY-22, INL will continue to develop methods to adapt rodlets with instrumented endcaps and will evaluate alternate sealing methods, which are anticipated to reduce the complexity of the Halden assemblies, for example through the use of a Conax fitting with a grafoil seal.

Thermocouple modeling showed the sensitivities to attachment/junction geometry, wire size, and boiling film thickness on measured temperature and resultant uncertainty. This work will continue and will provide the basis to analyze thermocouple attachments that are capable of being reliably reproduced on both fresh fuel specimens out of the hot cell environment and thermocouple attachments on previously irradiated fuel in the hot cell environment. A more complete understanding of the biases present due to the attachment and thermohydraulic conditions will support correction factors of the data and therefore more precise temperature measurements. This work is expected to continue in FY-22.

Space allocation for advanced refabrication and re-instrumentation remains a significant challenge. The preferred solution is the installation of a dedicated refabrication and re-instrumentation shielded cell within the TREAT Experiment Support Building. In support of this, conceptual design activities were continued of the EPIC shielded enclosure such that upon funding availability, project execution can begin immediately.

References

Idaho National Laboratory, Boise State University. Dhakal, S., Bateman, A., Hone, L., Jaques, B. “Microstructural Investigation of Thermocouple Attachment Strategies,” (unpublished manuscript, September 30, 2020), PDF file.

Idaho National Laboratory. 2021. “Conceptual Summary of EPIC System.” TEV-4341, Idaho Falls.

International Atomic Energy Agency. 2009. “Post-irradiation Examination and In-pile Measurement Techniques for Water Reactor Fuels.” IAEA-TECDOC-CD-1635, IAEA, Vienna. https://www-pub.iaea.org/MTCD/publications/PDF/TE_1635_CD/PDF/TECDOC_1635.pdf

Jensen, C., D. Wachs, N. Woolstenhulme, S. Hayes, G. Povirk, and K. Richardson. 2018. “Post-Halden Reactor Irradiation Testing for ATF: Preliminary Assessment and Recommendations.” INL/EXT-18-46101, Idaho National Laboratory. https://doi.org/10.2172/1484700.

Patnaik, S. 2020. “Comparative analysis of temperature dependent properties of commercial nuclear fuel pellet surrogates undergoing cracking: A review”, Ceramics International 46: 24765–24778. https://doi.org/10.1016/j.ceramint.2020.06.266.

Jensen, C., Condie, K., Woolstenhulme, N., Unruh, T., Larsen, E., Skifton, R., Calderoni, P., Svoboda, J. 2017. “Cladding Thermocouples for Transient Irradiation Experiments.” INL-EXT-17-43444 (Appendix D), Idaho National Laboratory.

Tsuruta, T. and Fujishiro, T. 1984. “Evaluation of Thermocouple Fin Effect in Cladding Surface Temperature Measurement during Film Boiling.” Journal of Nuclear Science and Technology 21(7): 515–527. https://doi.org/10.3327/jnst.21.515.

Tszeng, T.C. and Saraf, V. 2003. “A Study of Fin Effects in the Measurement of Temperature Using Surface-Mounted Thermocouples.” ASME Journal of Heat Transfer 125(5): 926–935. https://doi.org/10.1115/1.1597622.